Coral Reefs (2019) 38:467–488
https://doi.org/10.1007/s00338-019-01802-y

REPORT

High-resolution habitat and bathymetry maps for 65,000 sq. km of Earth's remotest coral reefs

Sam J. Purkis[1] · Arthur C. R. Gleason[1] · Charlotte R. Purkis[2] · Alexandra C. Dempsey[3] · Philip G. Renaud[3] · Mohamed Faisal[4] · Steven Saul[5] · Jeremy M. Kerr[6]

Received: 12 December 2018 / Accepted: 4 April 2019 / Published online: 19 April 2019

Abstract With compelling evidence that half the world's coral reefs have been lost over the last four decades, there is urgent motivation to understand where reefs are located and their health. Without such basic baseline information, it is challenging to mount a response to the reef crisis on the global scale at which it is occurring. To combat this lack of baseline data, the Khaled bin Sultan Living Oceans Foundation embarked on a 10-yr survey of a broad selection of Earth's remotest reef sites—the Global Reef Expedition. This paper focuses on one output of this expedition, which is meter-resolution seafloor habitat and bathymetry maps developed from DigitalGlobe satellite imagery and calibrated by field observations. Distributed on an equatorial transect across 11 countries, these maps cover 65,000 sq. km of shallow-water reef-dominated habitat. The study represents an order of magnitude greater area than has been mapped previously at high resolution. We present a workflow demonstrating that DigitalGlobe imagery can be processed to useful products for reef conservation at regional to global scale. We further emphasize that the performance of our mapping workflow does not deteriorate with increasing size of the site mapped. Whereas our workflow can produce regional-scale benthic habitat maps for the morphologically diverse reefs of the Pacific and Indian oceans, as well as the more depauperate reefs of the Atlantic, accuracies are substantially higher for the former than the latter. It is our hope that the map products delivered to the community by the Living Oceans Foundation will be utilized for conservation and act to catalyze new initiatives to chart the status of coral reefs globally.

Keywords Coral reef · Global Reef Expedition · Remote sensing · Habitat maps · Bathymetry · Accuracy assessment

Topic Editor Andrew Hoey

✉ Sam J. Purkis
spurkis@rsmas.miami.edu

[1] CSL – Center for Carbonate Research, Department of Marine Geosciences, Rosenstiel School of Marine and Atmospheric Science, University of Miami, Miami, FL 33149, USA

[2] Sea from Space Inc., Miami, FL 33133, USA

[3] Khaled bin Sultan Living Oceans Foundation, Annapolis, MD 21403, USA

[4] Michigan State University, Lansing, MI, USA

[5] Arizona State University, Phoenix, AZ, USA

[6] Guy Harvey Oceanographic Center, Halmos College of Natural Sciences and Oceanography, Nova Southeastern University, Dania Beach, FL 33004, USA

Introduction

Humans have been damaging reefs since they first started to interact with them (e.g., Pandolfi et al. 2003; McClenachan et al. 2017), but it is only in the last 40 yrs, or so, that impacts such as overfishing, pollution, and climate change have precipitated their global collapse (Jackson et al. 2001; Bellwood et al. 2004). Targeted intervention can reverse this demise using tools ranging from marine protected areas to reef restoration, but to be effective, it is necessary to understand the location of Earth's reefs and their status. For this reason, there is a compelling urgency to generate public-domain reef maps to guide effective coral reef conservation. Between 2006 and 2015, the Khaled bin Sultan Living Oceans Foundation under the auspices of their Global Reef Expedition (hereafter 'KSLOF-GRE') completed field research for one of the

largest coral reef studies in history, visiting a global transect of remote shallow-water reef sites (Fig. 1). The primary goals of the GRE were to map and characterize coral reef ecosystems, identify their status and major threats, examine factors affecting their resilience, and to promote local and regional conservation efforts through data sharing, outreach, and education. A key stipulation of the endeavor was that the Living Oceans Foundation was invited by each host nation into their territorial waters. By operating under invitation, it was deemed that the chances of nourishing local conservation efforts would be maximized. Further to this aim, every effort was made to include local scientists, managers, educators, as well as representatives from not-for-profit organizations, as part of the shipboard party. Many of these efforts have been described in high-level post-cruise reports (e.g., Bruckner et al. 2016; Purkis et al. 2017, 2018), documentary films (e.g., Barrat 2013, 2014, 2015, 2016), and scientific papers (see bibliography at www.livingoceansfoundation.org/publications/scientific-articles—accessed 11/27/2018). With the exception of the Red Sea surveys (Bruckner et al. 2011), however, little has been published on the methods used or accuracy of the KSLOF-GRE remote sensing products. Such is the overall purpose of this paper.

The KSLOF-GRE employed remotely sensed imagery along with contemporaneous field data to produce both

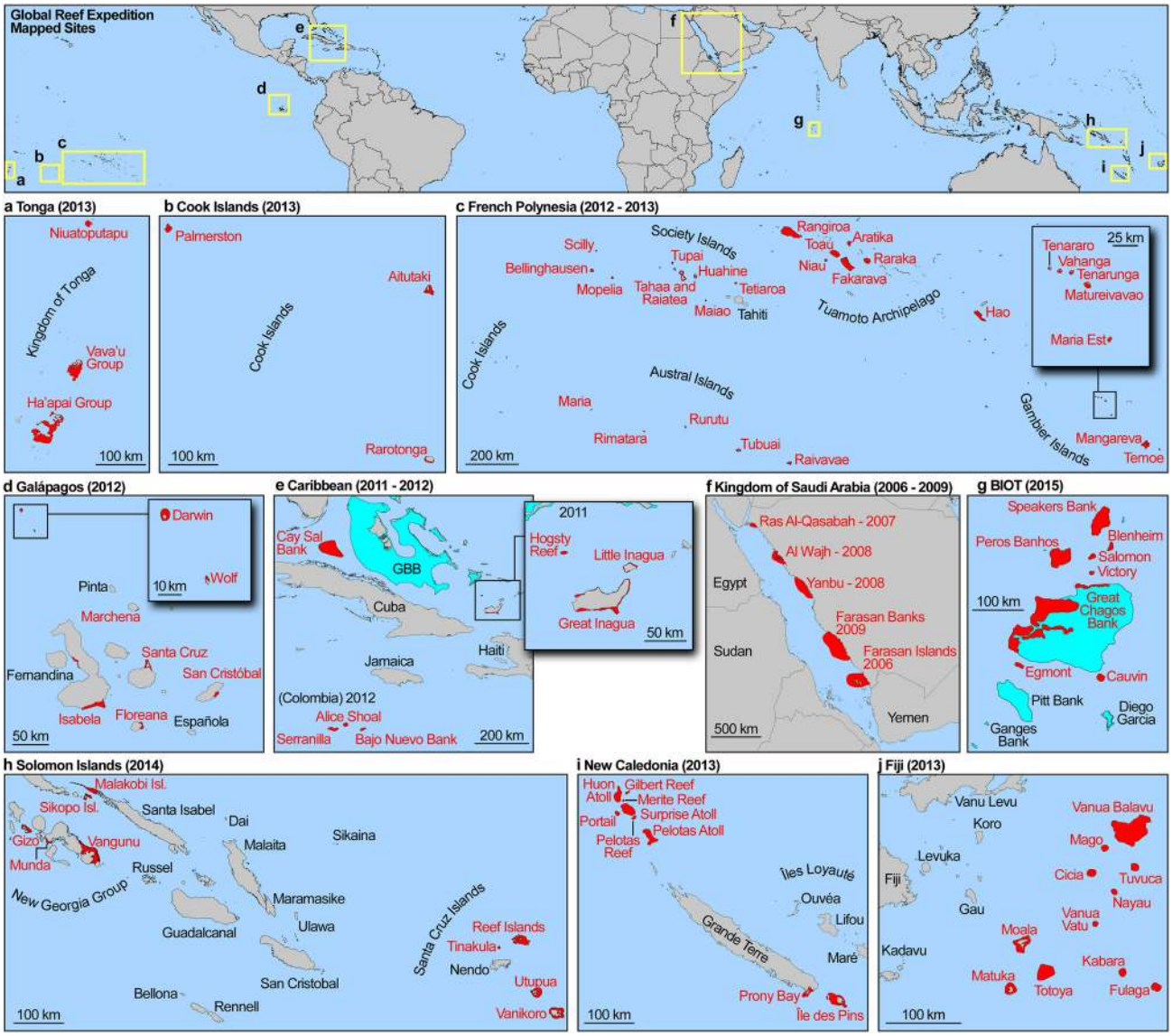

Fig. 1 **a–j** Location of the sites visited on the Khaled bin Sultan Living Oceans Foundation Global Reef Expedition where habitat and bathymetric maps were produced. Red polygons emphasize extent of mapping and encompass a total area of 65,000 sq. km of habitat situated shallower than 25 m water depth. Accompanying site names in red also. GBB in **e** abbreviates Great Bahama Bank. North is top in all maps; scales as noted

habitat maps and bathymetry at 2 m spatial resolution over an area of 65,000 sq. km. This area corresponds to coral reefs found in water shallower than 25 m. The completed work reflects the remarkable increase in accuracy of satellite-derived reef maps over the past 20 yrs and represents an important milestone toward mapping all of Earth's reefs at meter-scale spatial resolution.

Early remote sensing studies of coral reefs used government-operated sensors such as Landsat (e.g., Ahmad and Neil 1994; Andréfouët et al. 2001; Purkis et al. 2002; Naseer and Hatcher 2004) or SPOT (Satellite Pour l'Observation de la Terre; Loubersac et al. 1991; Capolsini et al. 2003). Although the 20–30 m pixel sizes of those sensors were considered high resolution for the time and were adequate to give the gist of seabed character, results using those data were incapable of capturing the heterogeneity of a typical reef environment as it would be experienced in situ. This shortcoming was largely overcome with the launch of IKONOS with 4 × 4 m pixels in the visible spectrum in 2000, followed by QuickBird with 2.4 × 2.4 m pixels in 2001, both of which were swiftly assigned to mapping reefs, albeit over areas of just a few hundred square kilometers (Andréfouët et al. 2003; Purkis, 2005; Hernández-Cruz et al. 2006; Purkis et al. 2006; Rowlands et al. 2008). More recent progress has been incremental and led by the WorldView series of satellites which offer visible-spectrum spatial resolutions between 1 and 2 m, two orders of magnitude smaller pixels than Landsat or SPOT of a generation ago. Beyond enhanced spatial resolution, the WorldView program delivers data in eight spectral bands, of which five are water penetrating, facilitating improved separation of seabed types and more accurate bathymetry derivation (Collin and Hench 2012; Goodman et al. 2013; Roelfsema et al. 2014, 2018; Glynn et al. 2015; Hedley et al. 2016; Warren et al. 2016; Kerr and Purkis 2018; Purkis 2018).

Although orbital sensors are now able to image Earth with spatial and spectral resolutions that could only be achieved using aircraft a decade ago, it is only recently that reef-mapping projects have started to tackle regional scales, as opposed to individual or small collections of reefs at specific locations. Computational limitations somewhat explain this local focus; regional image datasets are large and laborious to classify, not to mention complicated by broad variations in environmental conditions, such as tides, waves, and water clarity. The lack of research funds allocated to global mapping projects is an equal culprit, however. A small number of reef-mapping programs have, nevertheless, made the important jump to regional audits suitable for countrywide marine spatial planning initiatives. These programs can be categorized as to whether they deliver maps at Landsat-type resolution—that is, with minimum mapping units (MMUs) measured in hundreds of square meters—versus WorldView-type resolution, which is at least one order of magnitude finer.

There have been two regional-scale reef-mapping programs in the first category (Landsat-scale spatial resolution). First was the Biogeography Reef-Mapping Program of the US National Oceanic and Atmospheric Administration (NOAA) which was limited to US territorial waters and tendered at the minimum mapping unit of 1000 m^2 (Monaco et al. 2012). Second, and of similar resolution because it was developed from Landsat imagery, was the near-global reef database compiled by the United Nations Environmental Programme-World Conservation Monitoring Center (UNEP-WCMC). The Millennium Coral Reef-Mapping Project (Andréfouët et al. 2006) was the dominant constituent here.

There have also been two regional-scale reef-mapping programs in the second category (meter-scale spatial resolution). The first program to deliver meter-resolution reef maps at regional scales was the KSLOF-GRE and is the focus of this paper. The second program in this category is a recently launched initiative called the Allen Coral Atlas (www.allencoralatlas.com—accessed 03/07/2019). This endeavor aims for global coverage, is funded by Microsoft co-founder and philanthropist Paul Allen, and is utilizing satellite imagery provided by Planet Labs. The methods employed are based on work by Roelfsema et al. (2018) in the Great Barrier Reef. To date, the Allen Coral Atlas has completed various reef globally, including Heron Island (Australia), Karimunjawa (Indonesia), Kayankerni Reef (Sri Lanka), Moorea (French Polynesia), Lighthouse Reef (Belize), and West Hawai'i (USA.). All these data are accessible through the project's Web portal—www.allencoralatlas.com/atlas (accessed 03/11/2019). The KSLOF-GRE builds forward from earlier programs by providing coverage of much of Earth's major reef provinces, as accomplished by the Millennium Mapping Program, but at meter scale. Furthermore, the work conducted by KSLOF through the GRE might be considered as complimentary to new initiatives, such as the Allen Coral Atlas, by providing insight as to how field assessments and benthic habitat mapping can be scaled regionally.

Global Reef Expedition

The KSLOF-GRE simultaneously examined reef geomorphology, habitat, and satellite-derived bathymetry. Bathymetry is traditionally partnered with habitat maps because it has been demonstrated to hold predictive power over several ecologically important aspects of the reef system, such as the use of rugosity to forecast the diversity and biomass of reef fish (Purkis et al. 2008; Mellin et al. 2009; Knudby et al. 2011). Bathymetry maps are also the primary

input to the calculation of local hydrodynamic exposure (e.g., Purkis et al. 2012a, b; Callaghan et al. 2015).

The underlying philosophy of the KSLOF-GRE was to marry meter-resolution remote sensing and ground verification with traditional field surveys of reefs, such as those which have been continuously developed since 1998 by the Atlantic and Gulf Rapid Reef Assessment (AGRRA) Program (Ginsburg et al. 2000). AGGRA, and its expansive partner network, provides a standardized assessment of key structural and functional indicators that can be applied to reveal spatial and temporal patterns of reef condition. Based on a modified version of the AGRRA protocols, the KSLOF-GRE used SCUBA-diver surveys to systematically collect data at multiple depths for all visited sites to quantify, at a minimum, live coral and algal cover, as well as reef fish biomass and diversity.

From 2006 through 2009, the KSLOF-GRE operated along the Red Sea coastline of the Kingdom of Saudi Arabia during which four cruises were accomplished for the purpose of developing and refining the field and remote sensing protocols which would later be deployed globally. In this initial phase, reef geomorphology as it pertains to reef resilience was examined (Hamylton 2011; Riegl et al. 2012; Rowlands et al. 2014, 2016; Rowlands and Purkis 2015) alongside the sedimentology and Pleistocene development of the Red Sea (Purkis et al. 2010, 2015). Approximately 32,000 sq. km of shallow-water (< 25 m water depth) reef habitat and bathymetry were mapped from satellite and aircraft data (Fig. 1f), work which was summarized in a marine atlas of the Red Sea (Bruckner et al. 2011), a format which would later also be used to disseminate geographic products for the KSLOF-GRE. All of these data can be viewed on the interactive Living Oceans Foundation GIS Data Portal (https://maps.lof.org/lof—accessed 11/7/2018). Since it has already been published on extensively, the Red Sea component of the GRE is not the focus of this study and will not be considered further.

KSLOF-GRE surveys from 2011 to 2015 used a standardized survey protocol to collect baseline data on reef extent, habitat distribution, and health using a combination of diver, satellite, and other observations.

The aims of this paper are fourfold:

1. To emphasize the economies of scale that can be achieved by object-based interpretation of DigitalGlobe satellite data.
2. To highlight trends and patterns in error for the delineation of benthic habitats from orbit across diverse reef geomorphologies, seafloor types, water depths, and environmental settings.
3. To initiate a public repository of coral reef maps generated at appropriate scales to support regional-scale marine spatial planning initiatives.
4. To promote awareness of the KSLOF-GRE map products and initiate their widespread usage by the community.

Methods

Diver surveys for training data

The field component of the KSLOF-GRE was conducted between 2006 and 2015, and Table 1 provides an overview of the quantity of data acquired by country visited. For each of the 1000 individual reefs visited, the benthic cover of major functional groups and substrate type were assessed along 10 m transects using both diver-recorded observations, point-intercept counts, and photographic assessments. A minimum of four transects were completed at each dive site, and surveys were completed at 25, 20, 15, 10, and 5 m water depths. Via these methods, the following parameters were quantified: corals identified to genus, other sessile invertebrates identified to phylum or class, and six functional groups of algae. Reef fish surveys were also conducted at each dive site at depths stratified between 5 and 20 m via visual census as described by English et al. (1997). For more detail, the reader is directed to the Foundation's Field and Final Country Reports which are available online (www.livingoceansfoundation.org/publications/final-reports/—accessed 03/11/2019). These reports contain exhaustive lists of all sites and survey protocols.

Diver-collected data were used to aid in the definition of map classes, as described in "Definition of habitat map classes" section. In addition, the dominant habitat type was extracted from each dive site to serve as labeling (training) data for satellite mapping, as described in "Level 4 biological cover and Level 5 habitat maps" section. A total of 1240 dive sites across the KSLOF-GRE were treated in this way. This number of dives equates to approximately 15,000 hours of underwater data collection achieved by the > 200 scientists involved in the expedition.

Small-vessel surveys for training and validation data

A small vessel was used to collect several datasets at each of the $\sim$ 1000 visited reef sites. A total of 30-million tide-corrected single-beam sonar soundings were acquired throughout the KSLOF-GRE. These measurements were used to create the bathymetry maps ("Satellite-derived bathymetry maps" section). Additional ground-truth data were collected in the form of 2000 surficial sediment

Table 1 By-country summary of the field component of the Global Reef Expedition

Country	Fieldwork conducted	Area of coral reef mapped (sq. km)	Number of drop camera videos	Number of single-beam soundings	Number of dive sites
Red Sea	2006–2009	31,419	1759	2,711,903	164
Bahamas	2011	7801	1054	1,928,148	172
Colombia	2012	1103	446	364,771	69
BIOT	2015	3951	1205	4,459,966	115
Solomon	2014	2965	962	3,458,261	69
New Caledonia	2013	3024	1218	3,142,899	76
Galápagos	2012	1030	593	1,258,413	54
Fiji	2013	2542	987	3,037,823	91
French Polynesia	2012–2013	7802	1645	8,650,690	283
Cook	2013	1100	596	1,055,627	65
Tonga	2013	2322	724	1,602,931	82
Totals		65,059	11,189	31,671,432	1240

samples and 150 linear km of low-fold subbottom geophysical profiles obtained with a 5 kHz SyQwest Stratabox subbottom profiler—protocols for each detailed by Purkis et al. (2014). These datasets were used in conjunction with the diver data just described to help define habitat classes and segment geomorphological structures ("Definition of habitat map classes" and "Development of habitat maps" sections).

A total of 11,000 seabed videos were captured across all sites via a tethered SeaViewer 'drop' camera integrated with a differential global positioning system (dGPS). This video system allowed seabed observations to be obtained from the intertidal to approximately 50 m water depth at a frequency far exceeding that achievable via SCUBA. The drop camera videos were analyzed in the laboratory and used for map validation ("Accuracy assessment" section).

WorldView-2 satellite imagery

The KSLOF-GRE employed the DigitalGlobe Inc. WorldView-2 (WV2) satellite to image each visited reef site. The instrument images in eight multispectral bands with pixel widths of 1.85 m for images acquired with look angles $< 20°$ off-nadir coarsen to 2.07 m for look angles exceeding 20°. Pixel brightness values are digitally encoded with 11-bit radiometric resolution. WV2 is particularly adept at imaging the shallow seabed since five of the eight spectral bands are of sufficiently short wavelength to have meaningful penetration in water—these five are the coastal blue band (400–450 nm), blue (450–510 nm), green (510–580 nm), yellow (585–625 nm), and red (630 - 690 nm). Experience across the KSLOF-GRE suggested that under ideal conditions, the seabed could routinely be imaged for habitat mapping down to water depths of 25 m.

The tropics are often cloudy and therefore challenging to image. To address this difficulty, at least eight months prior to each of the 15 field missions, the WV2 was tasked to acquire imagery at look angles $< 15°$ off-nadir to minimize sun glint. At 1 month prior, all acquired imagery was purchased from DigitalGlobe Inc. and assembled to support mission planning and subsequent fieldwork. If insufficient cloud-free data had been obtained for mapping a given country, the sensor was tasked for an additional two-month post-cruise, to fill areas that remained stubbornly cloud contaminated. In this way, the majority of imagery was acquired within four months of fieldwork, but with a maximum differential of eight months. For large sites, such as the 6000 sq. km Cay Sal Bank (Bahamas—Fig. 1e), up to 50 individual WV2 acquisitions were assembled to deliver an image mosaic with $< 3\%$ cloud cover, which was the threshold deemed as the maximum tolerable for mapping. In many cases, cloud cover was further reduced by replacing individual cloud-contaminated areas with a portion of a cloud-free acquisition from an alternative date and equivalent tidal state, a process termed 'cloud patching.' Adjacent image scenes were selected to have a similar tidal state and equivalent water clarity.

Prior to mosaicking the individual scenes, each was processed to units of above-water remote sensing reflectance, which encompasses radiometric, solar geometry, and atmospheric correction, as described in detail by Kerr and Purkis (2018) and corrected for sun glint following Hedley et al. (2005). At this point, the processed satellite scenes were stitched into a mosaic using the image-processing

software ENVI (v. 5.4, Harris Geospatial Inc.), emergent areas identified using a threshold in the 860–1040 nm spectral band, and areas of deepwater identified also, defined as having $< 5\%$ reflectance in the 450–510 nm band (Fig. 2a). The remainder of the imagery was considered as potentially containing shallow-water habitat, defined as < 25 m water depth, and was passed forward to the mapping workflow (Fig. 2b–d).

Satellite-derived bathymetry maps

Bathymetry maps were derived for all the KSLOF-GRE sites via spectral derivation of water depth from WV2 satellite imagery (workflow detailed in Fig. 2b). These products served as stand-alone data layers, but were also utilized in the habitat-mapping workflow to partition each reef site into zones, which in turn were populated with a zone-specific suite of habitat classes. Stumpf et al. (2003) offer the most widely adopted empirical algorithm for extracting bathymetry from multispectral imagery. This solution uses a ratio of reflectance from two spectral bands which is tuned against known water depths to yield a bathymetry map. Motivated by the fact that this method does not exploit all five water-penetrating bands of WV2 and its successors, Kerr and Purkis (2018) evolved the algorithm via multi-linear regression of five bands, a solution which provided enhanced estimates of water depth. Their algorithm allowed viable bathymetric models

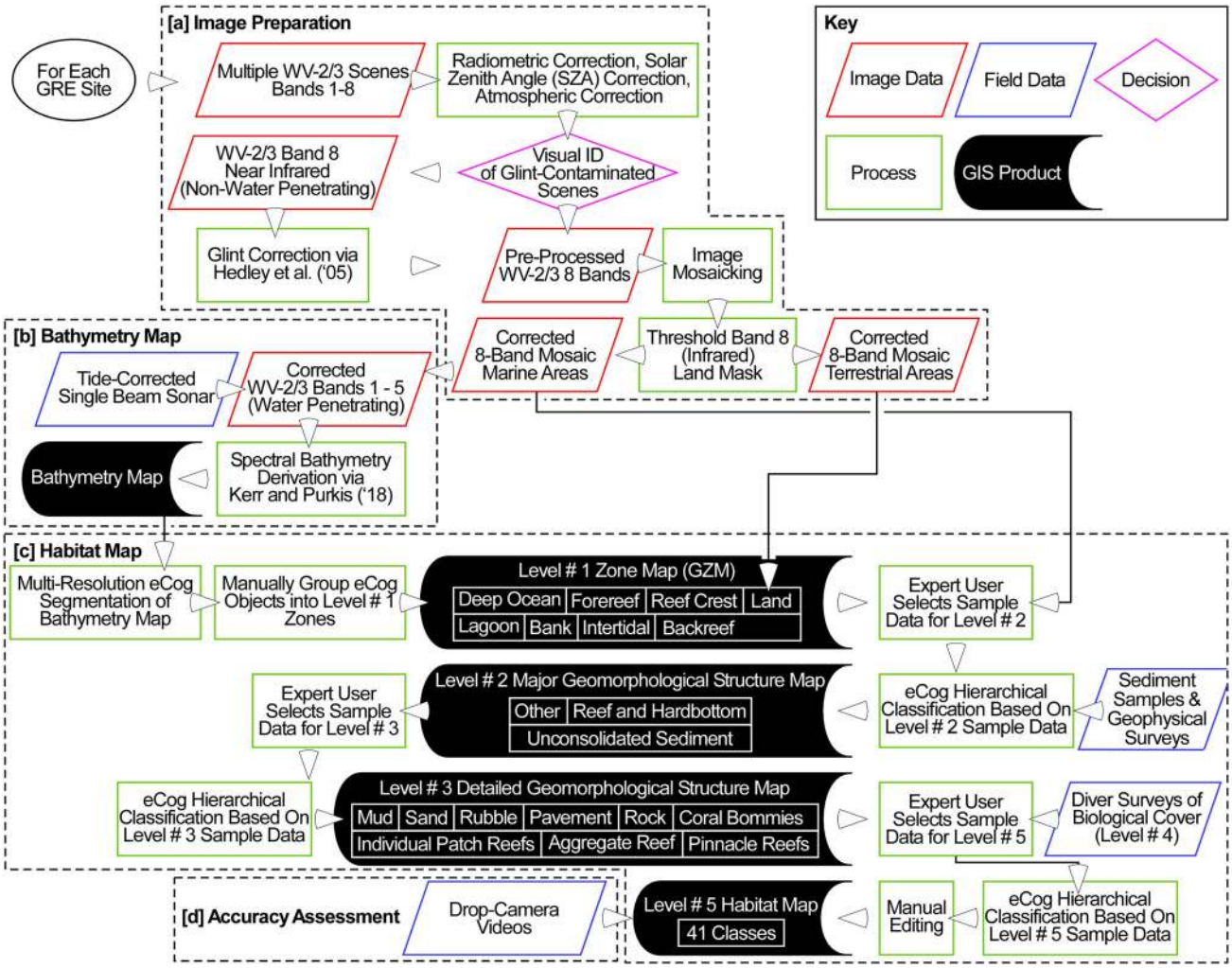

Fig. 2 Workflow for the production of bathymetry and benthic habitat maps. **a** Image preparation encompassed correction for solar, radiometric and atmospheric effects, and, if required, correction for sun glint also. Sites imaged by multiple satellite scenes were stitched into a seamless mosaic once these corrections had been implemented. The resulting mosaic was processed to yield a bathymetry map which was calibrated by sonar depth soundings (**b**). Via manipulation in eCognition software, the bathymetry map was used to create a map of reef zonation which was then combined with the multispectral image mosaic via hierarchical classification to yield a map of seabed habitat (**c**)—text for details. Finally, the accuracy of the habitat map was computed with reference to drop camera videos acquired in the field (**d**)

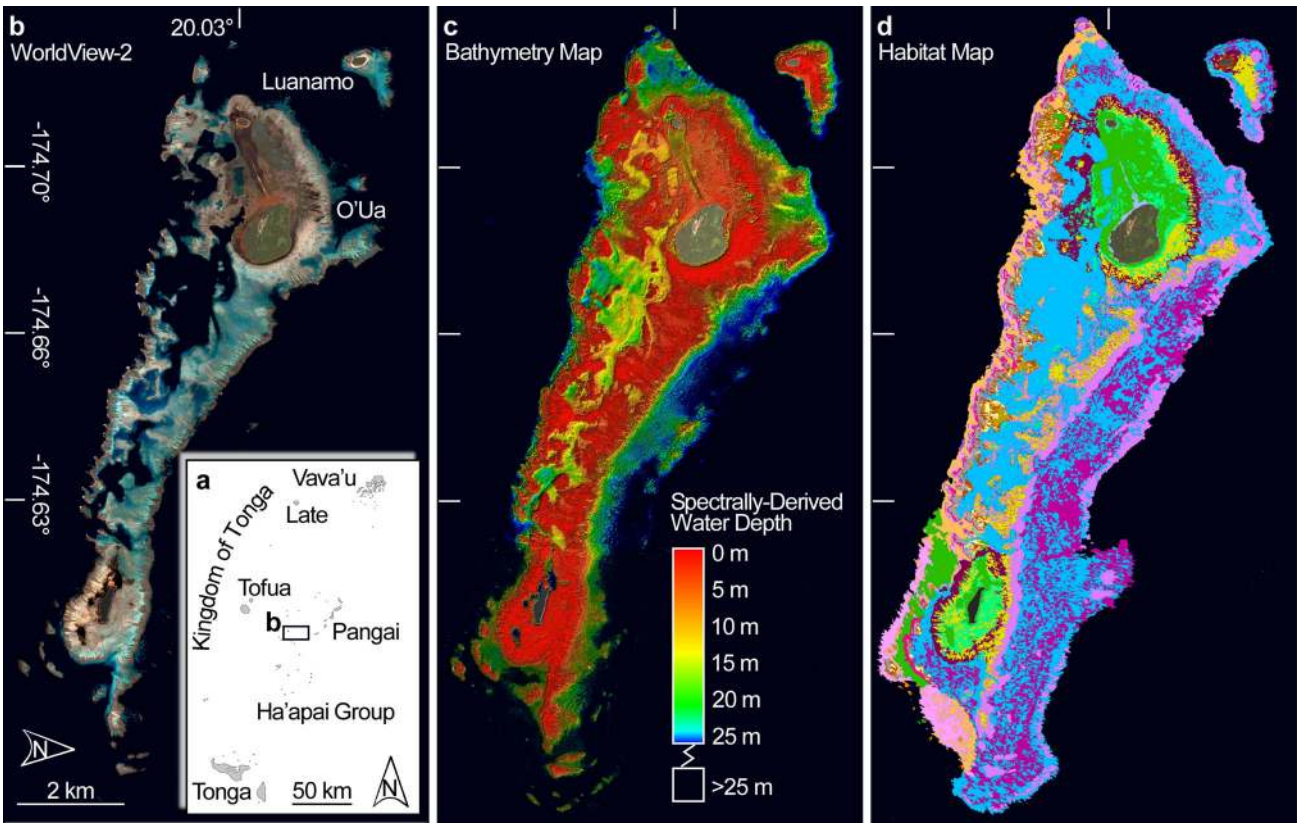

Fig. 3 Satellite-derived map products for O'Ua Island. **a** Location of O'Ua Island in the Ha'apai Island Group, Kingdom of Tonga. **b** Enhanced true-color WorldView-2 (WV2) image of O'Ua and surrounding reef systems. **c** Bathymetry map created via spectral derivation from the WV2 imagery calibrated by in situ sonar soundings. **d** Corresponding habitat map developed via object-based mapping in eCognition software. Colors in **d** correspond to those for the Level 5 map classes in Table 2. North is top

to be derived even in cases where ground truth via sonar was limited, and, under ideal conditions, even absent. Mapping of water depth for the KSLOF-GRE sites followed the Kerr and Purkis (2018) methodology and was calibrated by the sonar soundings described in "Small-vessel surveys for training and validation data" section. Bathymetry maps were masked below the 25-m-depth contour, as derived from sonar soundings.

Definition of habitat map classes

The KSLOF mapping endeavor built forward from two noteworthy regional-scale programs; the Millennium Coral Reef-Mapping Project (Andréfouët et al. 2006) and the NOAA Biogeography Reef-Mapping Program (Monaco et al. 2012). Although our habitat map classes differed from these predecessors, we adopted a hierarchical scheme which allows for cross-comparison (as also done by Roelfsema et al. 2018). The Landsat-derived maps of Andréfouët et al. (2006) delineated reef geomorphology, not habitat, though it was implied in many cases. For instance, class 'fore reef' in the Andréfouët et al. (2006) scheme describes location within the benthic system but, importantly, does not address substrate or cover type at that location. A fore reef environment can reasonably be anticipated to be coral-dominated, however. The NOAA effort (Monaco et al. 2012) also captured geomorphology, termed 'structure' in their nomenclature, but developed two additional map layers, 'biological cover' and 'geographic zone.' The former described dominant biota (e.g., live coral, seagrass, etc.), whereas the latter referred to the location of the benthic community within the system (e.g., reef crest, back reef, etc.). Unlike NOAA, the KSLOF-GRE products do not provide three map layers for each area, but the classification scheme was hierarchically arranged such that geomorphological structure, geographic zone, and biological cover can be separated if required. As described in "Development of habitat maps" section, this cross-compatibility is implicit to the way that the maps are created; a bathymetric map was initially interpreted into geographic zones (termed the 'Level 1' output), which was subsequently populated with increasing detail of geomorphological structure (Levels 2 and 3), before addition of biological cover recorded in situ (Level 4), to produce a final homologated Level 5 'habitat' map in which zone, structure, and cover are aggregated.

Table 2 Hierarchy of habitat classes utilized for satellite mapping

Level 1 (n = 8)	Level 2 (n = 3)	Level 3 (n = 11)	Level 4 (n = 12)	Level 5 (n = 36)	For Accuracy Assessment
Zone	**Major Geomorphological Structure**	**Detailed Geomorphological Structure**	**Biological Cover**	**KSLOF Aggregate Map Class**	**Consolidated Map Class (Non-Atlantic Class ID, n = 16) (Atlantic Class ID, n = 7)**
Land	Other	Land	Vegetated (Trees, Shrubs, Grass, etc.)	Terrestrial - Vegetated	Terrestrial (1, 1)
			Man-Made Structures (Roads, Buildings, etc.)	Terrestrial - Urbanized	
			Non-Vegetated (Soil, Rock, etc.)	Terrestrial - Unvegetated	
		Other	Water	Inland Waters	Inland Waters (2, N.A.)
Shoreline Intertidal	Unconsolidated Sediment	Mud	Mangroves	Intertidal - Mangroves	Intertidal Vegetation (3, 2)
			Salt Bushes and Grasses	Intertidal - Wetlands	
		Sand	Bare	Intertidal - Muds	Intertidal Sediment (4, 2)
				Intertidal - Beach Sands	
	Coral Reef and Hardbottom	Rock		Intertidal - Beach Rock	Intertidal Hardbottom (5, 2)
		Aggregate Reef	Macroalgae	Intertidal - Reef-Top Algal Mats	
Lagoon	Unconsolidated Sediment	Sand	Bare	Lagoon - Sediment Apron (Sediment Dominated)	Lagoonal Sediment with Variable Algal Cover (6, 3)
				Lagoon - Floor Barren	
			Macroalgae	Lagoon - Sediment Apron (Macroalgae Dominated)	
				Lagoon - Macroalgae on Sediment	
	Coral Reef and Hardbottom	Pinnacle Reefs	Live Coral	Lagoon - Pinnacle Reefs (Calcareous Red Algal)	Lagoonal Reef (7, 4)
				Lagoon - Pinnacle Reefs (Massive Coral Dominated)	
				Lagoon - Pinnacle Reefs (Branching Coral Dominated)	
		Aggregate Reef		Lagoon - *Acropora* Framework	
				Lagoon - Fringing Reefs	
		Individual Patch Reefs		Lagoon - Coral Bommies	
				Lagoon - Patch Reefs	
	-	-	-	Lagoon - Deep Water	Deep Water (8, 7)
Back Reef	Unconsolidated Sediment	Rubble	Algae	Back Reef - Rubble Dominated	Back Reef Sediment (9, 3)
		Sand	Bare	Back Reef - Sediment Dominated	
	Coral Reef and Hardbottom	Pavement	Bare or Turf Algae	Back Reef - Pavement	Back Reef Hardbottom (10, 5)
		Aggregate Reef	Live Coral	Back Reef - Coral Framework	
		Coral Bommies		Back Reef - Coral Bommies	
Reef Crest	Coral Reef and Hardbottom	Aggregate Reef	Coralline Algae	Reef Crest - Coralline Algal Ridge	Reef Crest Hardbottom (11, 4)
Bank / Shelf Escarpment	Coral Reef and Hardbottom	Aggregate Reef	Live Coral	Bank Shelf - Deep Fore Reef Slope	Bank / Shelf Hardbottom (12, 5)
Fore Reef	Coral Reef and Hardbottom	Aggregate Reef	Live Coral	Fore Reef - Shallow Fore Reef Terrace	Fore Reef Hardbottom (13, 5)
				Fore Reef - Shallow Fore Reef Slope	
	Unconsolidated Sediment	Sand	Bare	Fore Reef - Sand Flats	Fore Reef Sediment with Algae (14, 3)
(Multiple Zones)	Unconsolidated Sediment	Sand	Macroalgae	Dense Macroalgae on Sediment	
			Seagrass	Dense Seagrass Meadows	Seagrass (15, 6)
Deep Ocean	-	-	-	Deep Ocean Water	Deep Water (16, 7)
Other	-	-	-	Clouds	-

For each site, Level 1 classes were developed from a bathymetric map, Levels 2 and 3 were generated via hierarchical classification within eCognition software and Level 4 constituted in situ seabed observations of biological cover. Homologating Levels 1 through 4 delivered the KSLOF 36-class scheme (Level 5). *Colors* for the Level 5 classes correspond to those used in the example habitat maps (Figs. 3, 4, 5, 6). Map accuracy was assessed against 16 consolidated classes for all non-Atlantic sites and seven classes for Atlantic sites (final column). Consolidation of the Level 5 classes was required for accuracy assessment because of the reduced level of detail that can be extracted from underwater video—text for details. Each consolidated class was given a class ID which spans 1 through 16 for the non-Atlantic sites (emphasized in *red*, final column) and 1 through 7 for the Atlantic classes (*black*). These IDs were used in the error matrices (Table 3). The reduction in the number of Atlantic consolidated classes was achieved by further grouping the non-Atlantic classes. For instance, non-Atlantic consolidated classes '10 Back Reef Hardbottom,' '11 Reef Crest Hardbottom,' '12 Bank/Shelf Hardbottom,' and '13 Fore Reef Hardbottom' were further consolidated to a single class, '6 Reef,' in the Atlantic. Note that the class 'Inland Waters' was not represented in the Atlantic

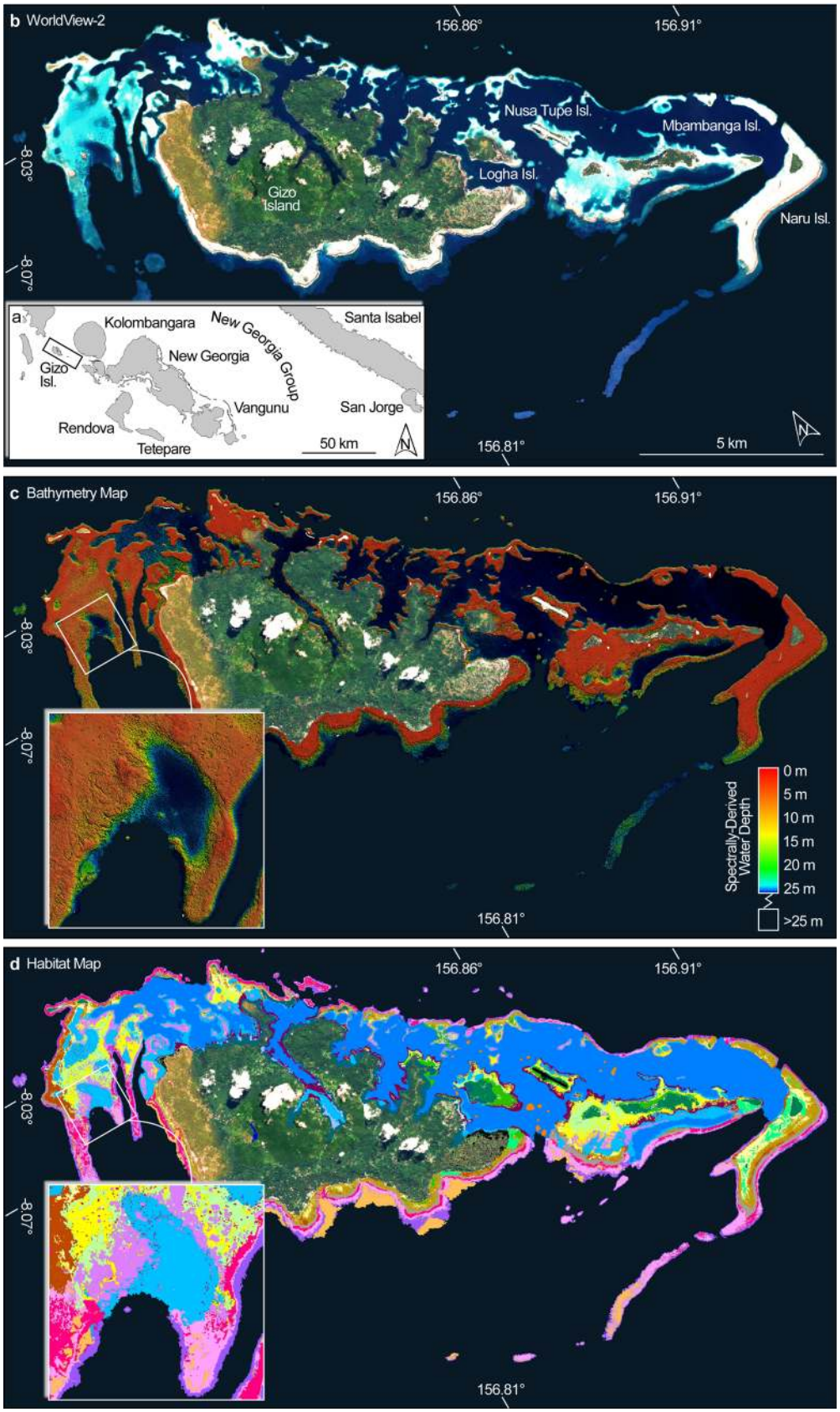
b WorldView-2
156.86°
156.91°
Nusa Tupe Isl.
Mbambanga Isl.
Logha Isl.
Gizo Island
Naru Isl.
-8.03°
-8.07°
a
Kolombangara
New Georgia Group
Santa Isabel
New Georgia
Gizo Isl.
Vangunu
San Jorge
Rendova
Tetepare
50 km
156.81°
5 km
c Bathymetry Map
Spectrally-Derived Water Depth
0 m
5 m
10 m
15 m
20 m
25 m
>25 m
d Habitat Map

◀**Fig. 4** Satellite-derived map products for Gizo Island, Solomon Islands. **a** Location of Gizo Island in the New Georgia Group. **b** Enhanced true-color WorldView-2 (WV2) image of Gizo and surrounding reef systems. **c** Bathymetry map created via spectral derivation from the WV2 imagery calibrated by in situ sonar soundings. **d** Corresponding habitat map developed via object-based mapping in eCognition software. Colors in **d** correspond to those for the Level 5 map classes in Table 2. North as indicated in **a**

The combination of reef zone, geomorphological structure, and biotic cover resulted in 36 habitat classes used across the Red Sea, Pacific, and Indian Oceans (Table 2). In the Atlantic, the same scheme was used, but not all combinations of zone, geomorphology, and cover were found in this ocean basin; only 25 of the classes were represented in the Atlantic maps. For example, there was no difference defined between 'lagoon' and 'back reef' in the Atlantic sites visited by the GRE. The description of these classes should make intuitive sense based on their zone, structure, and cover (Table 2), but there are also lengthy descriptions and example photographs for each class in the field reports previously published by KSLOF (see, for example, Bruckner et al. 2016).

Development of habitat maps

The KSLOF-GRE used eCognition software (v. 5.2, Trimble Inc.) to segment the WV2 imagery into polygons that were then labeled by zone, structure, and ultimately habitat class. In contrast to pixel-based classifiers, which assign image pixels to map classes based on their spectral content (Purkis and Klemas 2011), eCognition follows an object-based approach (Knudby et al. 2011; Phinn et al. 2012; Purkis et al. 2012a, b, 2014; Roelfsema et al. 2013, 2014, 2018; Zhang et al. 2013; Warren et al. 2016). In a workflow termed 'hierarchical classification,' edge-detection routines are used to segment imagery into eCognition 'objects,' which are precincts of the image set with similar spectral and/or textural attributes. These objects are subsequently assigned into one of several map classes based on rules which consider spectral/textural signatures, shape, and contextual relationships with surrounding classes.

Whereas recent progress has been made to automate the assignment of objects to map classes, such as by Saul and Purkis (2015) using multinomial logistic discrete choice models, we found the accuracy of the automated assignments to be consistently lower than that delivered manually by an expert user. For this reason, we elected to use manual assignment of eCognition objects to map classes in our workflow for the production of the KSLOF-GRE habitat maps (Fig. 2). The workflow required four steps to handle preprocessing of the satellite imagery, derivation of a bathymetry map, development of a habitat map, and accuracy assessment (Fig. 2a–d, respectively). This section deals solely with developing the habitat map (Fig. 2c); the other three steps are described in their corresponding sections.

Level 1 zone map

A Level 1 zone map for each site was created using eCognition by applying a multi-resolution segmentation algorithm to the bathymetry map. This algorithm, because it was described in detail by Baatz and Schäpe (2000), will only be treated briefly here. The general concept of multi-scale image segmentation is to subdivide an image set into objects with spectral and/or textural homogeneity. The solution proposed by Baatz and Schäpe (2000) considers this task an optimization problem. In the first step, every image pixel is considered a separate image object. Each object is then visited iteratively and merged with its neighbors to form larger (multi-pixel) objects. With each iteration, the merging decision is based on local homogeneity criteria describing the similarity of adjacent image objects. In a process similar to the annealing function described by Purkis et al. (2012b), a cost function is tracked as each merge is conducted and objects cease to be further amalgamated at the point that the function ceases to reduce.

To create the Level 1 map, the multi-resolution segmentation was deployed on the bathymetry map, which has pixel values enumerating water depth. Once segmented, an expert user manually grouped the resulting image objects that correspond to five reef zones (lagoon, back reef, fore reef, reef crest, and shelf), plus two zones encompassing terrestrial areas (land and intertidal), and deep ocean (Table 2). The upshot of this process was a Level 1 zone map.

Levels 2 and 3 geomorphological structure maps

The next step toward the final habitat map was the delineation of geomorphological zones which were first crudely defined (Level 2) and then refined in more detail (Level 3). For the Level 2 map, the inputs were (a) the Level 1 reef zone map produced from bathymetry and (b) the multispectral WV2 image mosaic. First, for each Level 1 zone, the multispectral imagery was segmented via the multi-resolution method of Baatz and Schäpe (2000). Second, in a process termed 'labelling' and with reference to the surficial sediment samples and geophysical profiles acquired in the field, the expert user manually selected image objects and attributed them as belonging to one of the three Level 2 geomorphology classes (unconsolidated sediment, coral reef and hardbottom, or other; see Table 2).

Table 3 Error matrices for the consolidated classes used to assess the classification accuracy for Atlantic (a) and non-Atlantic sites (b)

a. Atlantic Sites

Classified Data (i.e. Predicted) \ Ground-truth Data (i.e. Actual)	Reef (4)	Hardbottom (5)	Sediment with Macroalgae (3)	Seagrass (6)	User's Accuracy
Reef (4)	**34**	0	4	0	**89%**
Hardbottom (5)	13	**534**	64	49	**81%**
Sediment with Macroalgae (3)	1	25	**224**	46	**76%**
Seagrass (6)	0	10	29	**236**	**86%**
Producer's Accuracy	**71%**	**94%**	**70%**	**71%**	

Overall Accuracy = 81%, Kappa = 71%, Tau = 72%

b. Non-Atlantic Sites

Classified Data (i.e. Predicted) \ Ground-truth Data (i.e. Actual)	Lagoonal Sediment with Algae (6)	Lagoonal Reef (7)	Back Reef Sediment (9)	Back Reef Hardbottom (10)	Reef Crest Hardbottom (11)	Bank / Shelf Hardbottom (12)	Fore Reef Hardbottom (13)	Fore Reef Sediment with Algae (14)	Seagrass (15)	User's Accuracy
Lagoonal Sediment with Algae (6)	**621**	25	9	0	0	1	2	2	4	**93%**
Lagoonal Reef (7)	188	**1153**	18	2	1	0	3	3	1	**84%**
Back Reef Sediment (9)	1	4	**160**	1	0	0	1	3	0	**94%**
Back Reef Hardbottom (10)	6	0	24	**124**	0	0	2	0	0	**79%**
Reef Crest Hardbottom (11)	0	0	0	0	**1**	0	0	0	0	**100%**
Bank / Shelf Hardbottom (12)	0	0	0	0	0	**462**	4	2	0	**99%**
Fore Reef Hardbottom (13)	3	0	2	0	0	1	**804**	46	0	**94%**
Fore Reef Sediment with Algae (14)	0	0	0	0	0	8	19	**85**	0	**76%**
Seagrass (15)	2	2	1	0	0	0	0	0	**30**	**83%**
Producer's Accuracy	**76%**	**97%**	**75%**	**98%**	**50%**	**98%**	**97%**	**59%**	**86%**	

Overall Accuracy = 90%, Kappa = 87%, Tau = 89%

Columns capture the ground-truth data and rows the classified data. The integers in parentheses after the consolidated class names (*black* for Atlantic, *red* for non-Atlantic sites) are consistent with the class IDs developed in the final column of Table 2. Correctly classified points (i.e., where the ground truth and habitat map were in agreement) lie along the major diagonal of the matrices. Off-diagonal positions reflect errors of omission and commission, as captured by the producer's and user's accuracies, respectively

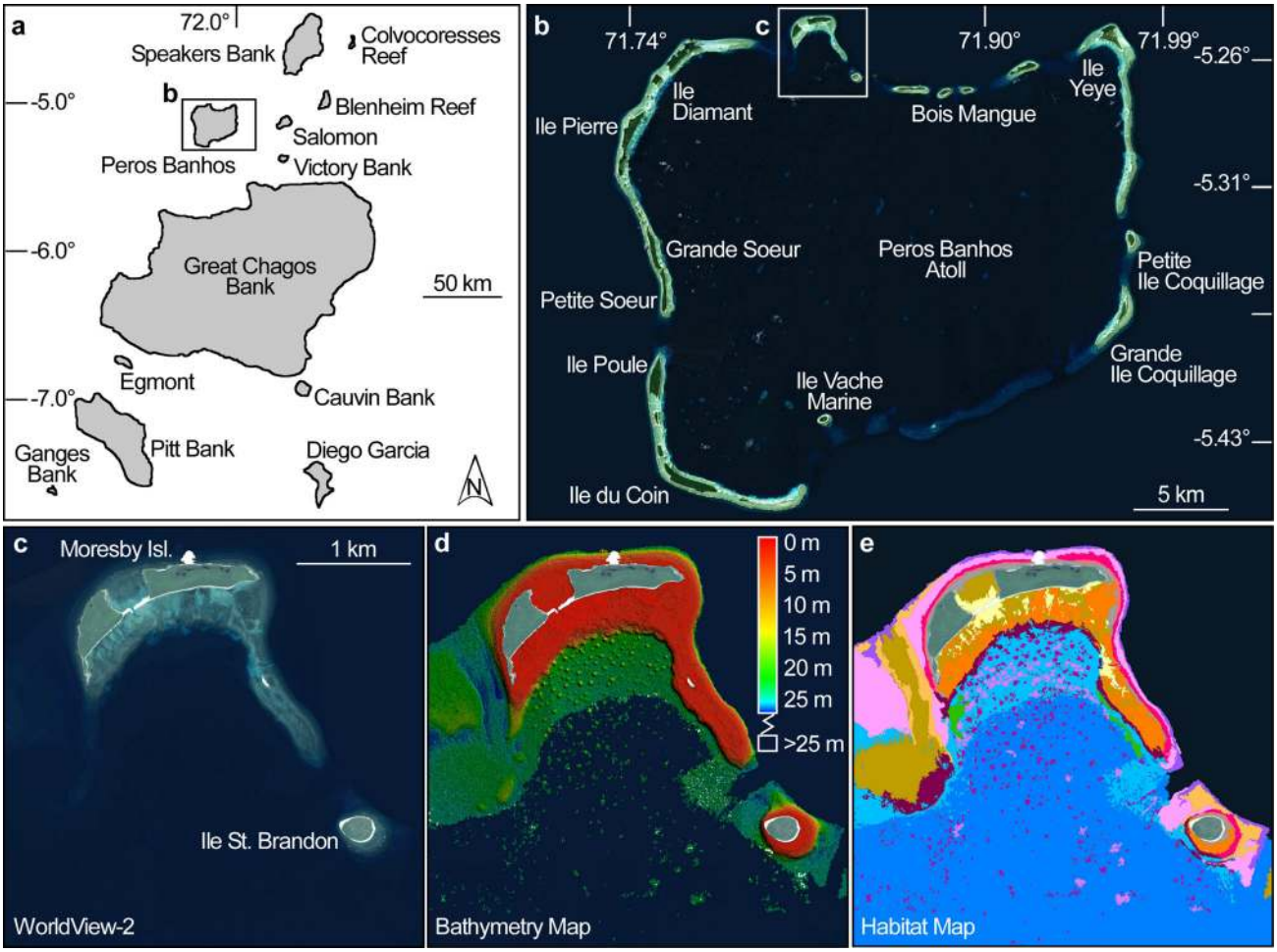

Fig. 5 Satellite-derived map products for Moresby Island, Peros Banhos Atoll. **a** Location of Peros Banhos Atoll in the Chagos Archipelago—British Indian Ocean Territory. **b** Enhanced true-color WorldView-2 (WV2) image of Peros Banhos, with focus on the reefs fringing Moresby Island (**c**). **d** Bathymetry map created via spectral derivation from the WV2 imagery calibrated by in situ sonar soundings. **e** Corresponding habitat map developed via object-based mapping in eCognition software. Colors in **e** correspond to those for the Level 5 map classes in Table 2. North is top

Third, based on these user-defined training sets for each Level 2 class in each Level 1 zone, eCognition was used to classify all of the objects in the image set into geomorphological structures based on spectral, textural, and neighborhood parameters. The upshot of this process was a map of major geomorphological structure primarily split into unconsolidated sediment-dominated areas (spectrally bright and texturally homogeneous) and coral reef and hardbottom-dominated areas (spectrally dark and texturally heterogeneous). Note that by conducting this process independently within each Level 1 zone, the bias introduced by varying bathymetry across the satellite imagery was mitigated by the fact that each zone occupies a limited range of water depths. This was important because the rapid attenuation of light by water tends to override the subtle spectral differences between reef habitats (e.g., Purkis 2005).

The detailed geomorphological structure maps (Level 3) were produced in the same way as in the preceding step, but the imagery was re-segmented on the basis of the Level 2 classes and for each, the expert user applied labels for the 11 Level 3 classes defining seabed character (mud, sand, rock, etc.; see Table 2) and in the case of reefs, their morphological type (pinnacle versus aggregate, etc.; see Table 2). The advantage of conducting this segmentation based on the Level 2 classes was a radical reduction in computational overhead since subsets of the overall image mosaic were segmented separately. As before, the user manually developed these labels with reference to known points on the ground visited during fieldwork, and, again, eCognition was used to classify the unlabeled image objects based on their similarity to the training set.

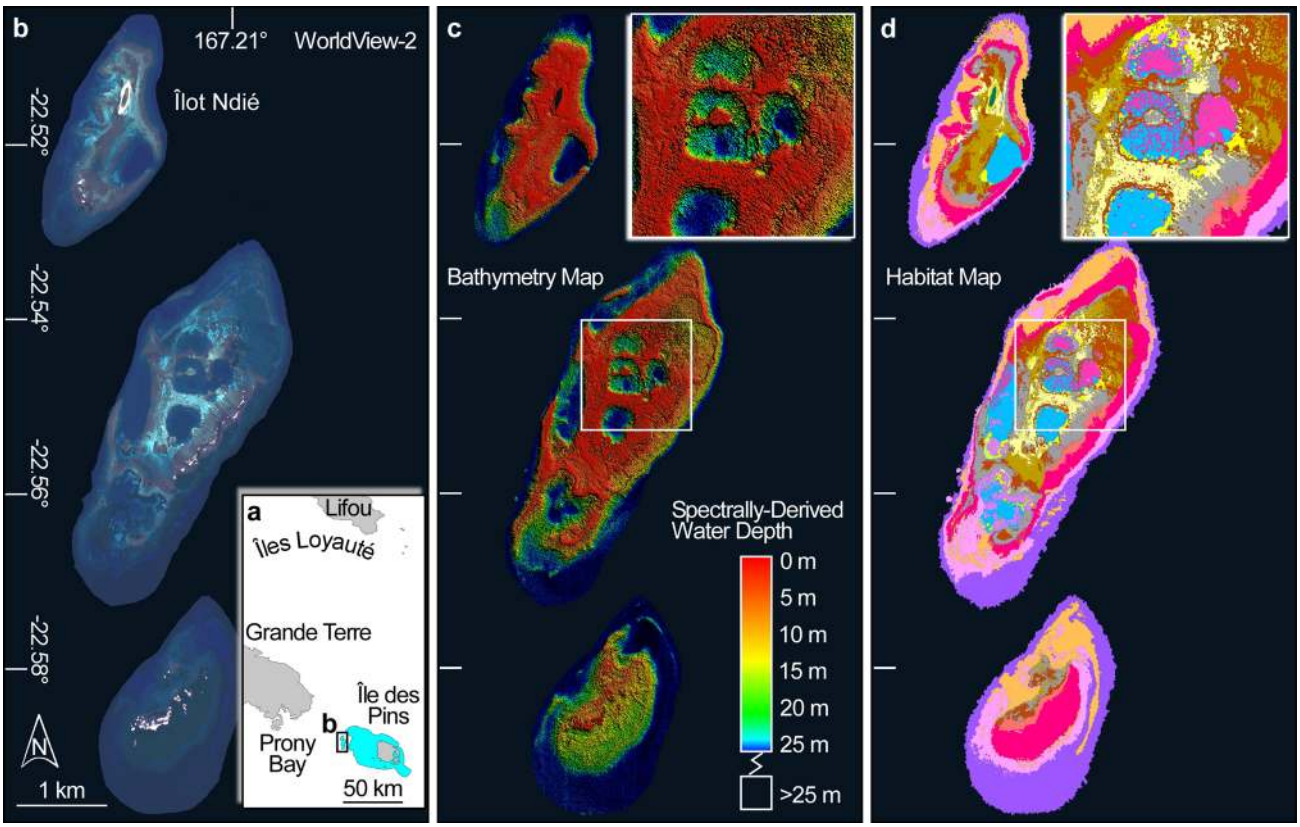

Fig. 6 Satellite-derived map products for a series of isolated reef platforms offshore Île des Pins. **a** Location of Île des Pins, part of the Île Loyauté, New Caledonia. **b** Enhanced true-color WorldView-2 (WV2) image of the reef complex. **c** Bathymetry map created via spectral derivation from the WV2 imagery calibrated by in situ sonar soundings. **d** Corresponding habitat map developed via object-based mapping in eCognition software. Colors in **d** correspond to those for the Level 5 map classes in Table 2. North is top

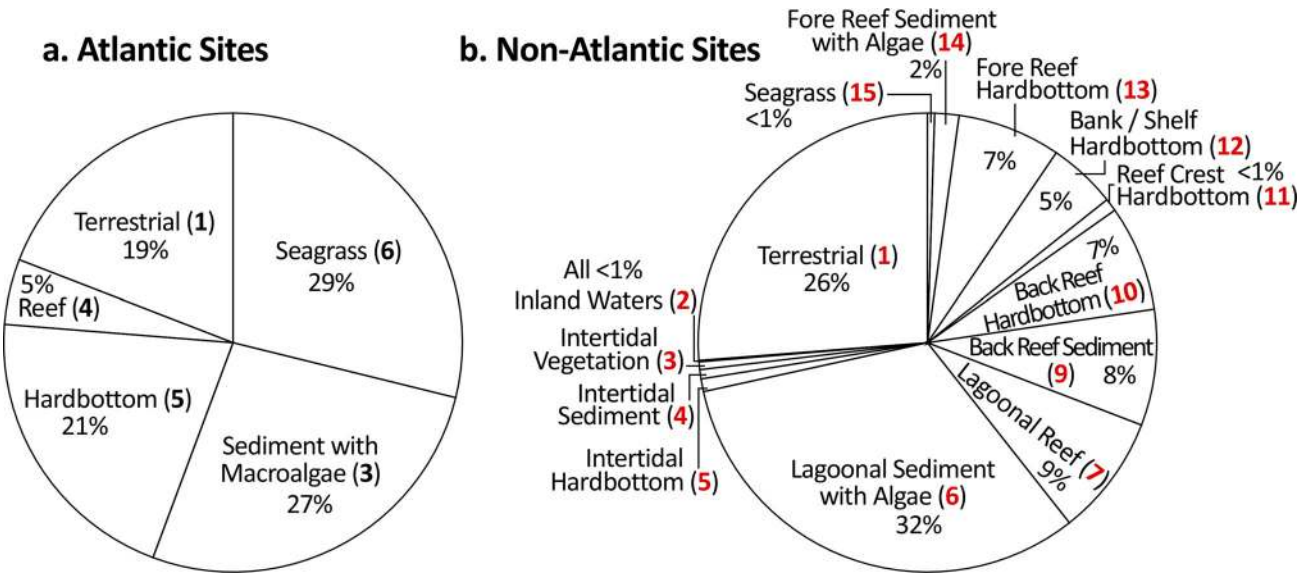

Fig. 7 Proportional composition by consolidated habitat class for the Atlantic (**a**) and non-Atlantic sites (**b**). The integers in parentheses after the class names (black for Atlantic, red for non-Atlantic sites) are consistent with the class IDs developed in the final column of Table 2. The habitat maps for the Atlantic sites were characterized by high proportional coverage of seagrass but low occurrence of reef substrate. The opposite trend was seen for sites outside the Atlantic

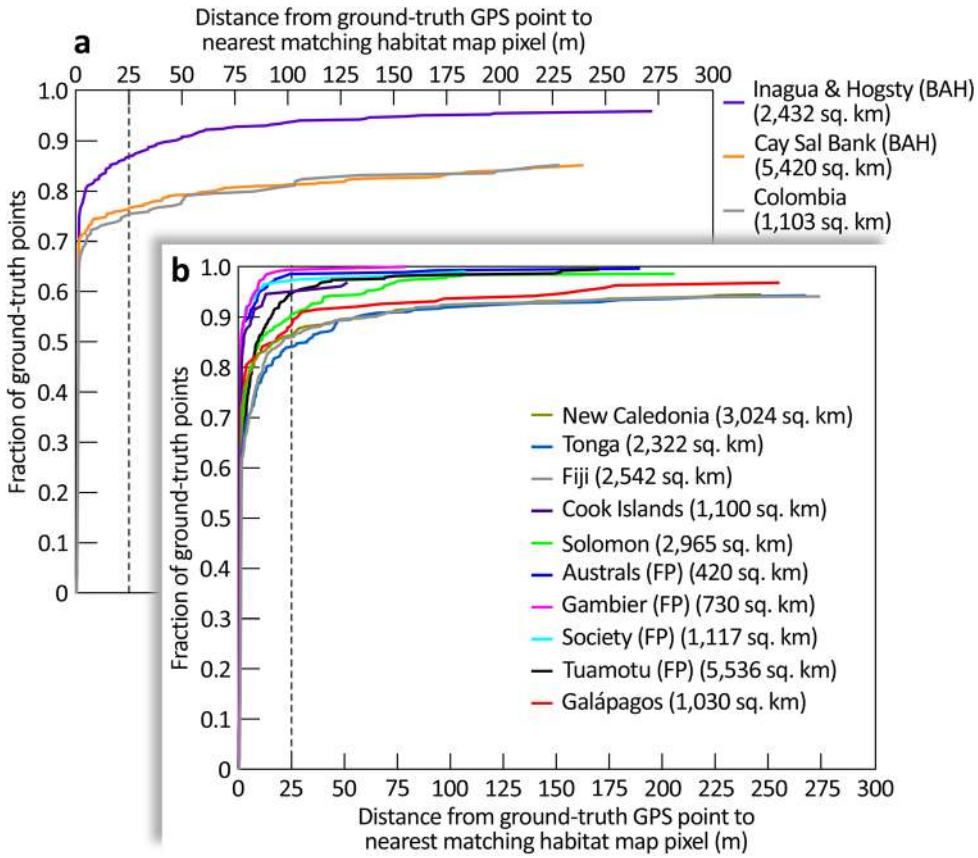

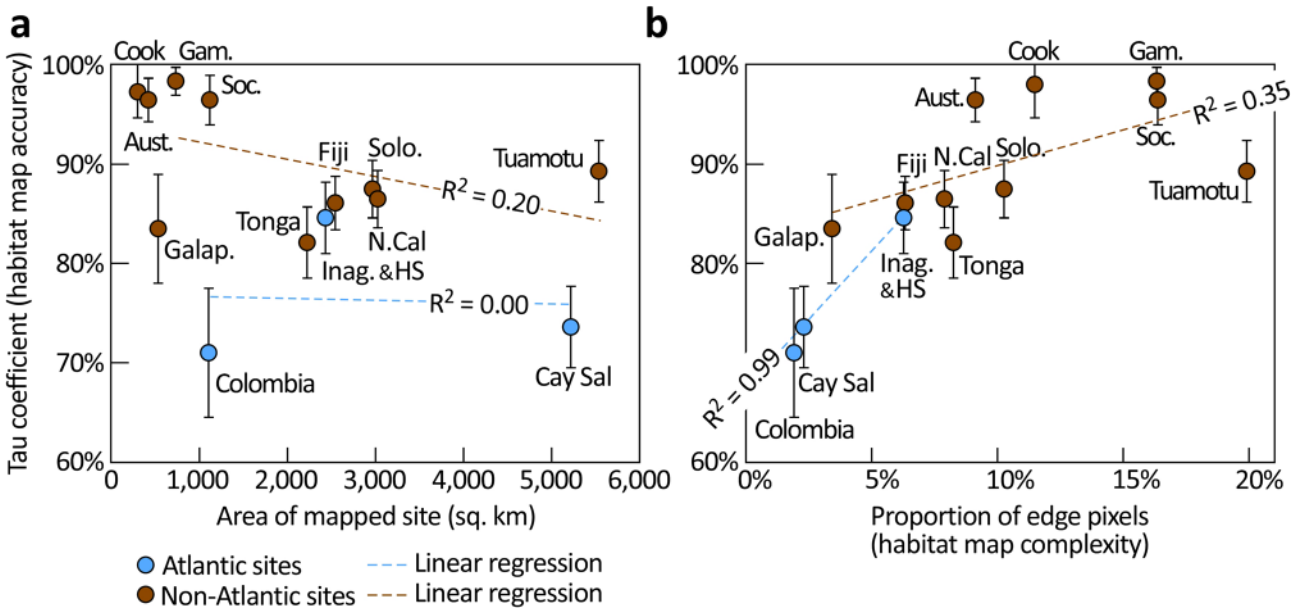

Fig. 8 Cumulative distribution functions for the Atlantic (**a**) and non-Atlantic (**b**) sites charting the probability (*y*-axis) of encountering correctly classified habitat map pixels at increasing lag distances (*x*-axis) from the GPS-constrained ground-truth points. As a guide to these plots, for the Galápagos habitat map there was a 90% probability of encountering a correctly classified pixel within 25 m of a ground-truth point (broken vertical line). For the Gambier map, meanwhile, there was a 99% probability at the same lag distance. Note that the accuracy of the Atlantic habitat maps was lower than the non-Atlantic sites. 'BAH' denotes 'Bahamas' and 'FP' for 'French Polynesia.' Area of shallow-water habitat (< 25 m depth) mapped for each site in parentheses

Fig. 9 Relationship between habitat map accuracy and map area (**a**) and map complexity (**b**). Map accuracy was quantified by the Tau coefficient and complexity via the proportion of edge pixels (text for details). In both plots, the (linear) correlation was computed for Atlantic (*blue broken line*) and non-Atlantic sites (*brown*). No correlation was observed between map accuracy and area for either grouping of sites. Only low correlation ($R^2 = 0.35$) exists between accuracy and map complexity for non-Atlantic sites. These variables are highly correlated for the Atlantic maps ($R^2 = 0.99$), meanwhile, but with only three sites in this ocean basin, the relationship should be not be overly emphasized. Site abbreviations in plots as follows: Galap. = Galápagos, Inag. and HS = Inagua and Hogsty, N. Cal = New Caledonia, Solo. = Solomon Isl., Aust. = Austral Isl., Gam. = Gambier

Level 4 biological cover and Level 5 habitat maps

In the final step in the mapping workflow, field observations of biological cover (termed 'Level 4' data) were convolved with the geomorphology map to yield a map of habitat (e.g., Figs. 3d, 4d, 5d, 6d). This step was again achieved via application of the multi-resolution segmentation algorithm (Baatz and Schäpe 2000), but this time, the Level 3 classes were individually segmented and, again with reference to field data, the user manually selected labels for objects characterized by the 12 Level 4 classes of biological cover. Again, eCognition was used to classify the remaining unattributed image objects on the basis of similarity to the training set. As laid out in Table 2, each object, now classified according to benthic cover, was attributed with the addition of its zone and geomorphological structure, which varied by location within the image set, as defined by the previously created Level 1 and 2 maps, respectively. As an example, an image object describing a patch reef in the lagoon would be reattributed as 'Lagoon–Patch Reef,' and so on. This reattribution process delivered the 36 'aggregate classes' of the final habitat map. To complete the map, boundaries existing between image objects of the same class were dissolved such that areas of a single habitat type were encompassed by a single polygon. At this stage, and again with reference to the diver observations, the evolving map was examined by an expert user and any obvious errors corrected in a process termed 'contextual editing' (as originally proposed by Mumby et al. 1998). To complete the process, the finished habitat map was exported as an ESRI shapefile for further analysis in a geographic information system (GIS).

Accuracy assessment

Accuracy assessment of the habitat maps was conducted using error matrices (Story and Congalton 1986; Congalton 1991) with reference to the 5106 dGPS-positioned seabed videos captured using a tethered 'drop' camera that remained independent from the map-making workflow. These drop camera videos had three advantages for the purposes of accuracy assessment: a large sample size, wide, consistent coverage across the entirety of the GRE sites, and independence from the training/labeling process of map creation. The drop camera dataset suffered a few limitations as well. First, some habitat types were undersampled due to physical constraints navigating the vessel. Second, the limited field-of-view of the camera created difficulties discriminating certain habitat classes. Third, there was some geographic uncertainty in camera location due to the tether length and the horizontal field-of-view. The first two of these limitations were addressed by eliminating or consolidating certain map classes for the purposes of accuracy assessment. The third was addressed by considering the neighborhood around each drop camera point using a technique we call 'lagged accuracy.' It is important to emphasize that field-operation logistical planning helped reduce these uncertainties by accounting for wind, as well as current magnitude and direction, when deploying the camera and capitalizing on precise boat handling techniques by the highly skilled skipper. This allowed us to accurately position and 'fly' the tethered camera over each habitat sampled.

Terrestrial habitat classes were impossible to sample with the drop camera, for obvious reasons. Thus, the accuracy of terrestrial habitat classes was not quantitatively assessed for these maps. Nevertheless, we assume that the maps are very accurate for a consolidated 'terrestrial' class (i.e., consolidated map Class #1; Table 2), since segmenting land versus marine habitats is straightforward with the infrared channels of satellite imagery. Intertidal and reef crest classes also proved difficult to sample, due to their extremely shallow depths at the islands surveyed. Only two reef crest videos and no intertidal videos were captured. Thus, the accuracy for intertidal classes was not assessed and fore reef crest was insufficiently sampled to draw strong conclusions. To put this limitation in perspective, however, intertidal and reef crest classes were each found to have $< 1\%$ of the total number of classified pixels (Fig. 7). Therefore, their omission from the accuracy assessment is unlikely to change overall conclusions about classifier performance.

The limited field-of-view of the drop camera prevented the discrimination of many of the fine details between Level 5 classes (Table 2). For instance, the videos were adequate to classify the seabed in general as a 'Lagoonal Reef,' but the field-of-view was inadequate to resolve whether a given lagoonal reef was only 10 m in diameter, or smaller, which would correspond to the Level 5 map class 'Lagoon–Coral Bommies,' versus a much larger patch, which would be a Level 5 'Lagoon–Pinnacle Reef.' To compensate for this discrepancy in scale between the satellite data and the ground-truth data, we grouped the 36 Level 5 classes into a smaller number of 'consolidated classes' (Table 2). For most sites around the world, 16 consolidated classes were used, reflecting different combinations of geographic zone and substrate. In the Atlantic, however, geographic zone was not as easy to define, so additional classes were consolidated in the Atlantic, reducing the total to seven for those sites.

Overall, producer's and user's map accuracies were computed for each site using the consolidated classes (Table 2) via the error matrix approach (Story and Congalton 1986). In addition, the Kappa (Congalton 1991) and Tau (Ma and Redmond 1995) coefficients were computed to quantify the degree to which the accuracy of each map

was better than random chance. Equal prior probability was used for calculating Tau because no a priori information on class probability was used in the hierarchical segmentation. It should be noted that the accuracies quoted in the error matrices (Table 3) are for the consolidated classes and cannot be extrapolated to speak to the accuracy of the individual classes prior to their consolidation.

Map accuracy as assessed via standard error matrices does not allow for geographic offsets between the habitat map and reference data. Such offsets are often unavoidable, however, and stem from the many vagaries of setting an exact position on the ocean during fieldwork. Sources of positional error include GPS inaccuracies, diver observations not made exactly beneath the position recorded when entering the water, and the drift of the tethered 'drop' camera away from the boat. These offsets might reasonably be expected to routinely exceed the 1.85 m pixel width of the WorldView satellite, with the result that the ground-truth data are not perfectly registered with the habitat map. Furthermore, with a horizontal field-of-view, as was the case with the drop camera used for this study, the video data are directional, which can have just as great an impact as positional uncertainty. Imagine the camera positioned on an edge between two classes; the class assigned to that ground-truth point would depend on the direction in which the camera was orientated, even if the camera position did not change. Whereas such offsets might legitimately be considered as inaccuracies for habitat maps produced on a local scale, we consider them to be acceptable when mapping across hundreds of thousands of sq. km of Earth's remotest reef systems. Thus, we wanted a way to assess accuracy that would account for uncertainty in the relative position of ground truth to satellite data.

To sensibly address geographic uncertainty in camera location, we used a metric called 'lagged accuracy' which, for each ground-truth point, collates the cumulative probability of encountering pixels mapped as the same class attributed to the assessment point, for lag distances between 0 and 300 m offset from that point, in all Cartesian directions. Providing that map pixels of the class sought exist within the specified lag distance around the accuracy assessment point, the cumulative probability of encounter will rise as a function of increasing lag, with the rate of that rise dictated by the density of pixels of that class in the queried portion of the habitat map. Of course, it is unreasonable to take the existence of a map pixel within the search radius with the same class assignment of that of the accuracy assessment point to justify scoring the map as accurate. Indeed, for large lag distances, the correct assignment will be recognized even if the queried habitat map is random. Hence, it is necessary to set sensible thresholds in both lag distance and cumulative probability that might rationally indicate that a positioning error has precluded an exact match at the location of the accuracy assessment point. While there are no precise answers, we felt 25 m was a sensible threshold for the accuracy of a regional-scale map used to support marine spatial planning.

Patterns of habitat classification accuracy

To explore possible causes of habitat map error, the per-site Tau coefficients (a measure of map accuracy) were cross-plotted against mapped area and the complexity of the habitat maps (Fig. 9). Doubtless, the KSLOF-GRE dataset allows for all sorts of analysis of the spatial patterns among reef systems around the globe, and it is our hope that it will be used for such in the future. The present goal, however, was simply to check for broad and systematic patterns related to habitat classification accuracy.

There are many ways to quantify scene complexity. One of the simplest is to count the proportion of edge pixels, i.e., those which border a different class. Edge pixels are good metrics for assessing habitat classification because they are affected by a combination of class variety, spatial arrangement, and pixel mixing (Heydari and Mountrakis 2018). Furthermore, accuracy has sometimes been shown to decrease with increasing proportion of edge pixels (Heydari and Mountrakis 2018). Checking whether this pattern held for the KSLOF-GRE was valuable because datasets with a sufficient number of scenes with varying complexity to test this are rare.

Results

The KSLOF generated benthic habitat maps and bathymetry over a total of 65,000 sq. km during the 10 yrs of the Global Reef Expedition. Examples of these products are reproduced here for the Pacific and Indian Oceans (Figs. 3, 4, 5, 6). The entire digital dataset can be explored on the KSLOF GIS data portal (https://maps.lof.org/lof—accessed 11/7/2018). As demonstrated by Figs. 3, 4, 5, and 6, the object-based workflow used for mapping seabed character scaled to tens of thousands of sq. km, while maintaining high spatial fidelity.

Sites in the Atlantic were comprised of $< 5\%$ reef habitat, nearly 25% hardbottom, and 29% as seagrass (Fig. 7). Non-Atlantic sites, by contrast, contained $< 1\%$ seagrass and $> 15\%$ reef habitat. Even though biogeographic differences in benthic character were not the subject of this paper, these statistics underline the diversity of sites mapped using a common workflow across the KSLOF-GRE.

A quantitative assessment of classification error (Table 3) revealed the overall accuracy of the maps developed for the three Atlantic sites to be approximately

10% lower than that for the ten non-Atlantic sites (81% vs. 90%, respectively). The Kappa and Tau coefficients differed by nearly 20% between the Atlantic and non-Atlantic sites, however. Kappa and Tau both penalize the Atlantic results more than the other sites because of the fewer number of consolidated classes used to conduct the accuracy assessment in the Atlantic (4) versus elsewhere (9).

The producer's accuracies for the habitat classes in the Atlantic maps were approximately 70%, save for 'Hardbottom,' which was 94% (Table 3). Much of this discrepancy arose from confusion between macroalgal stands and seagrass meadows which occupied large swaths of the 6000 sq. km Cay Sal Bank (Fig. 1e). The user's accuracies for the Atlantic sites were generally higher than the producer's accuracies, ranging from 76% (Sediment with Macroalgae) to 89% (Reef).

Both producer's and user's accuracies for the 13 non-Atlantic sites were considerably higher than for the Atlantic. An outlier here was the class 'Reef Crest Hardbottom' (Producer's Accuracy = 50%, User's = 100%) which should be ignored as it was validated by a single ground-truth point, a function of the difficulty of safely navigating a small vessel across the shallow reef crest. Withstanding this class, the median producer's accuracy was 92% and user's accuracy was 89%, both reassuringly high values.

Cumulative distribution functions describing the lagged accuracy of the three Atlantic (Fig. 8a) and ten non-Atlantic sites (Fig. 8b) echoed the trend obvious in the error matrices (Table 3). The habitat maps for the Atlantic had lower accuracies than those developed for non-Atlantic sites. Maps created for Colombia and the Cay Sal Bank (Bahamas) were the worst performers here, with only a 75% probability of encountering a correctly classified pixel within 25 m of a ground-truth point (Fig. 8a). The maps for Great and Little Inagua, and Hogsty, were $\sim$ 10% better, but still underperformed the non-Atlantic sites. For these, the probability of encountering a correctly classified pixel within 25 m of the ground-truth data exceeded 90% for the Solomon Islands, the four mapped archipelagos in French Polynesia (Australs, Gambier, Society, and Tuamotu), and the Cook Islands. The probability at the same lag distance for the remaining sites (Tonga, Fiji, New Caledonia, and Galápagos) exceeded 85%. By a lag distance of 50 m, which is likely on the upper limit of what is useful for a regional-scale map product, the probability of encountering a correctly identified pixel exceeded 90% for all sites except Colombia and the Cay Sal Bank.

Map accuracy and area were uncorrelated for both the Atlantic and non-Atlantic sites (Fig. 9a). For the latter grouping, however, a low level of correlation (R^2 = 0.35) was observed between accuracy and complexity (Fig. 9b). The correlation between these parameters was strong for the three Atlantic sites (R^2 = 0.99), but the result is unreliable because of the small number of sites in this grouping.

Discussion

Regional-scale coral reef mapping from remote sensing has a role to play in the widening portfolio of intervention measures that are being mobilized against the reef crisis. Of these measures, the establishment of large-scale marine protected areas (MPAs) has been particularly effective (Sheppard et al. 2012; Toonen et al. 2013; Wilhelm et al. 2014). The Big Ocean Network (https://bigoceanmanagers.org—accessed 10/25/2018) provides a rule of thumb as to what constitutes 'large scale,' with their 17 member sites ranging in size from approximately 150,000 sq. km to nearly 2000,000 sq. km. Beyond large size, the success of an MPA rises if it is nested within a network of ecologically connected protected areas, which as a collective encompass a full range of critical habitats (Graham et al. 2008; Gleason et al. 2010). Designing ecological connectivity into MPA networks, however, requires careful consideration of available information on habitat distribution, larval dispersal patterns, adult movement ranges, and oceanography (Botsford et al. 2001; Gaines et al. 2003; Palumbi 2004). Marine spatial planning—MSP—(Douvere 2008) is a central component to balancing these and other considerations in the design of MPAs. Habitat and bathymetry maps lie at the base of the MSP workflow and are therefore critical to its success. With MPAs becoming ever larger, it is imperative that the mapping keeps pace.

Covering 65,000 sq. km and taking nearly a decade to complete, the KSLOF-GRE is the largest coherent reef-mapping program accomplished to date. The results from the GRE are presently being used to train the next generation of image classifiers which hold the potential to deliver truly global audits of reef status through time. As developed by Chirayath and Earle (2016) and Chirayath and Li (2019), the delineation of reef habitat via machine learning holds particular promise. Further, the goal to 'map once, use many ways' underpins and justifies the KSLOF-GRE and the archiving of its outputs in the public domain. As the expedition was planned, the Foundation was agnostic to the degree to which each host nation was conducting MSP. Instead, the philosophy was to deploy the KSLOF-GRE seafloor mapping program to stimulate the creation of national and regional databases and information systems containing essential coral reef environmental data, else contribute to these if they already existed.

Accuracy of the KSLOF-GRE habitat maps, as computed with the traditional error matrix approach (Story and Congalton 1986), varied from $\sim$ 70 to 90%. The technique used here of computing lagged accuracy, in addition to a

traditional error matrix, resulted in cumulative probability functions for each map class (Fig. 8) which grant the map user an alternative means of judging map quality. In some ways, lagged accuracy conveyed the same information as overall accuracy computed using a traditional error matrix approach. For example, the error matrices showed that Atlantic sites had lower overall accuracy, in general, than non-Atlantic sites (Table 3). This same result was also clear from plots of lagged accuracy (Fig. 8). In other ways, however, lagged accuracy complemented the error matrix approach with new information about the spatial distribution of errors. For example, the sites with the steepest slopes of the lagged accuracy curve in the 0–25 m spatial scale had the highest fraction of edge pixels (Tuamotu, Gambier, and Society). Conversely, those with the shallowest slope over that range had the fewest edge pixels (Colombia, Cay Sal, Galápagos). Thus, information about the relationships among patchiness, scale, and accuracy was contained in the lagged accuracy cumulative distributions. This is a topic to be examined further in the future.

Lagged accuracy also provides a thematic analog to familiar specifications for spatial accuracy. Horizontal spatial data accuracy is typically reported in the following form: '*X* meters (feet) horizontal accuracy at the 95% confidence level' (FGDC 1998). One could use lagged accuracy to report a thematic accuracy in an analogous form, for example: '*X*% thematic overall accuracy within *Y* meters horizontal lag.' Users could specify an acceptable spatial lag, *Y*, according to their needs. A manager planning marine protected areas across one million square km of ocean might acceptably tolerate a larger *Y* than, say, an engineer planning a dredging operation.

All KSLOF-GRE sites except Cay Sal and Colombia were found to have at least 85% thematic overall accuracy within 25 meters horizontal lag; Cay Sal and Colombia had 75% thematic overall accuracy within 25 m horizontal lag. If faced with developing a network of MPAs across hundreds of thousands of sq. km of tropical ocean, as has already been accomplished by the 17 member sites of the Big Ocean Network, access to maps which correctly position the occurrence of critical habitats such as coral reefs, seagrass meadows, and mangrove stands to within 25 m would be of huge benefit, especially considering that most of these protected areas were defined without any precise knowledge of the locations, size, and architecture of benthic habitat throughout their range.

The fact that, regardless of which accuracy metric was used, the Atlantic sites were $\sim$ 10% less accurate than those in the Pacific and Indian oceans was surprising because the diversity of seabed character is considerably lower in the Atlantic, and therefore fewer classes were used to map these sites. In contrast, several previous studies have shown that increasing the number of habitat classes decreases map accuracy (e.g., Andréfouët et al. 2003). One potential explanation for this inconsistency can be linked to the workflow used to produce the maps. Our workflow relied on a bathymetric map derived from satellite imagery to guide development of a Level 1 map of reef zones which was subsequently evolved to a Level 2 map of major geomorphic structure (Fig. 2). The sites considered outside the Atlantic were well poised for this approach as they were predominantly atolls with well-defined zones (fore reef, reef crest, lagoon, etc.). Once the seascape has been split into zones, the burden of mapping the habitats contained within them was eased because a limited number of benthic cover types were prescribed in advance for each zone (as detailed in Table 2). The Atlantic sites mapped by KSLOF-GRE were challenging to partition into reef zones, except for the diminutive Hogsty Reef, which is only 100 sq. km in area but atollic in morphology. The Level 1 zone map for the 5500 sq. km Cay Sal Bank, however, was more poorly defined because Cay Sal lacks platform-margin reefs and takes the form of a sediment-dominated flat-topped carbonate bank (Purkis et al. 2014). Thus, the Atlantic maps placed greater emphasis on correctly ascribing benthic cover across a large area, from a large quantity of potential biotic classes. We anticipate that this disjoint in our workflow explains the reduced accuracy of the Atlantic habitat maps. This said, the 81% overall accuracy for Atlantic maps falls in line with, or exceeds comparable studies conducted at much smaller spatial scales (e.g., Phinn et al. 2012; Zhang et al. 2013; Collin et al. 2014; Hedley et al. 2016; Roelfsema et al. 2018) and is therefore not deemed to be a limiting factor.

A regression of map accuracy and area yielded no (linear) correlation in the Atlantic and at most a slight inverse relationship for non-Atlantic sites (Fig. 9a). The lack of a relationship was reassuring and indicated that the workflow was not confounded by very large sites. The positive correlation observed between map accuracy and map complexity (Fig. 9b) was counterintuitive. Rather than accuracy decreasing with increasing map complexity, as previously documented for pixel-based approaches to classification (Andréfouët et al. 2003; Heydari and Mountrakis 2018), our object-based approach yielded increasing accuracy for more complex benthic systems. The explanation for this result might be due to pixel-based versus object-based classifiers, or due to the zone-based classification scheme used. Note, however, that the correlation between accuracy and complexity was high for the Atlantic sites but rather modest for the non-Atlantic sites. Thus, we feel this result can be most easily interpreted as another manifestation of the lowered performance of our workflow in the Atlantic sites where reef morphology is less well developed than outside the Atlantic.

Throughout our mapping endeavors, we found that some habitat types tended to be misclassified more often than others. For example, in the Atlantic, sediment with macroalgae was occasionally misclassified as hardbottom. Confusion existed too between seagrass and either sediment with macroalgae or hardbottom. Such errors are to be anticipated because of the spectral similarity of these classes (Hochberg and Atkinson 2003; Purkis 2005). For non-Atlantic sites, lagoonal sediment with macroalgae was sometimes misclassified as lagoonal reef, confusion which might variably be attributed to their spectral and textural similarity and the fact that turbidity in restricted atoll lagoons can be elevated (Kjerfve 1986). Forereef sediment with macroalgae was occasionally wrongly mapped as forereef hardbottom. In this case, the rapid downslope increase in water depth can likely be implicated as near-vertical morphology is challenging to image because of light attenuation and shadowing (Jay et al. 2017). Ways to more routinely separate live coral from macroalgae in multispectral imagery are of heightening importance given the large-scale regime shift of reefs to algal-dominated states (Graham et al. 2015; Hughes et al. 2017; Hempson et al. 2018).

The products discussed in this manuscript, and the spatial breath of coverage the KSLOF-GRE achieved, provide a major contribution to the science and management of coral reefs, and the ecosystem services they provide. Studies of this magnitude provide critical baseline data to benchmark the condition of reefs now, thereby enabling; (1) quantification of the rate and direction of future change at seascape scales, (2) enhanced understanding of how reefs should be managed to ensure their sustainability, and (3) documentation of how they change once management interventions are in place. Many countries visited during the GRE are Small Island Developing States, whose economies are wholly dependent on the submerged marine resources located within their EEZ. As such, resource management at the national level is critical to the local economies of these nations. In addition, most of the KSLOF-GRE sites are home to isolated villages of people (i.e., monthly ferry service and no airport) who are truly dependent on their adjacent reef environment for food security (Béné et al. 2016). Dissemination of the KSLOF-GRE mapping products and survey data to the host countries and communities provides the greatest opportunity for their use at both the national and local levels.

Coral reefs are icons of environmentalism because they have degraded so rapidly with causes easily linked to climate change and other human pressures. Despite iconic status, though, Earth's reefs have not been systematically mapped with the intensity of, for instance, tropical deforestation. This deficit means that even fundamental questions such as area covered by reefs globally are unknown. This includes the inability to formally assess coral reef health and status at country level. Though by no means covering every reef worldwide, the KSLOF-GRE covers a meaningful proportion of key reef provinces around the world and provides a baseline of their health prior to the 2017 mass bleaching event. According to Spalding et al. (2001), Earth's reefs cover nearly 285,000 sq. km, a figure which would suggest that the KSLOF-GRE mapping, which covers 65,000 sq. km, has characterized one-fifth of them. This proportion is tenuous, however, as the true global reef area is poorly constrained, not least because of the rarity of large-scale maps—a deficit which motivated this study. We hope that our large-scale maps will open new vistas of potential enquiry and motivate others to work toward a global reef audit. Many aspects of the reef crisis are presently intractable. We show that accurately mapping bathymetry and habitat at regional scale is not one of them.

Acknowledgements We owe a debt of gratitude to the host nations of the Global Reef Expedition who not only permitted our team to work in their countries, but also provided both logistical and scientific support. We are similarly indebted to the crew of the M/Y Golden Shadow, through the generosity of HRH Prince Khaled bin Sultan, for their inexhaustible help in the field. We thank Brett Thomassie and DigitalGlobe Inc. for their unwavering assistance over a decade of intense satellite image acquisition. The project would have been impossible without the 200+ scientists who participated in the Global Reef Expedition. We further thank Andy Bruckner, Luis Ramirez, and Bernhard Riegl for their sterling efforts at sea. The manuscript benefited greatly from comments by Acting Editor in Chief Andrew Hoey, Topic Editor Alastair Harborne, and two anonymous reviewers.

Compliance with ethical standards

Conflict of interest The authors declare that they have no conflict of interest.

References

Ahmad W, Neil DT (1994) An evaluation of Landsat Thematic Mapper (TM) digital data for discriminating coral reef zonation: Heron Reef (GBR). International Journal of Remote Sensing 15:2583–2597

Andréfouët S, Muller-Karger FE, Hochberg EJ, Hu C, Carder KL (2001) Change detection in shallow coral reef environments using Landsat 7 ETM+ data. Remote Sensing of Environment 78:150–162

Andréfouët S, Muller-Karger FE, Robinson JA, Kranenburg CJ, Torres-Pulliza D, Spraggins SA, Murch B (2006) Global assessment of modern coral reef extent and diversity for regional science and management applications: a view from space. In:

Proceedings 10th International Coral Reef Symposium 2:1732–1745
Andréfouët S, Kramer P, Torres-Pulliza D, Joyce KE, Hochberg EJ, Garza-Pérez R, Garza-Pérez R, Mumby PJ, Riegl B, Yamano H, White WH, Zubia M (2003) Multi-site evaluation of IKONOS data for classification of tropical coral reef environments. Remote Sensing of Environment 88:128–143
Baatz M, Schäpe A (2000) Multiresolution segmentation: an optimization approach for high quality multi-scale image segmentation. Angewandte Geographische Informationsverarbeitung XII 58. Wichmann-Verlag, Heidelberg, pp. 12–23
Barrat A, director (2013) Sharks of the coral canyon. Living Oceans Foundation
Barrat A, director (2014) Mapping the blue. Living Oceans Foundation
Barrat A, director (2015) Coral reefs: trouble in paradise. Living Oceans Foundation
Barrat A, director (2016) An ocean mystery: the missing catch. Living Oceans Foundation
Bellwood DR, Hughes TP, Folke C, Nyström M (2004) Confronting the coral reef crisis. Nature 429:827
Béné C, Al-Hassan RM, Amarasinghe O, Fong P, Ocran J, Onumah E, Ratuniata R, Van Tuyen T, McGregor JA, Mills DJ (2016) Is resilience socially constructed? Empirical evidence from Fiji, Ghana, Sri Lanka, and Vietnam. Global Environmental Change 38:153–170
Botsford L, Hastings A, Gaines S (2001) Dependence of sustainability on the configuration of marine reserves and larval dispersal distance. Ecological Letters 4:144–150
Bruckner A, Rowlands G, Riegl B, Purkis SJ, Williams A, Renaud P (2011) Khaled bin Sultan Living Oceans Foundation atlas of Saudi Arabian Red Sea marine habitats. ISBN-978-0-9835-611-1-8. 273 pp
Bruckner AW, Dempsey AC, Coward G, Saul S, Rauer EM, Heemsoth A (2016) Global Reef Expedition: Lau Province, Fiji. Final Report. Khaled bin Sultan Living Oceans Foundation, Annapolis, MD. 113p. ISBN: 978-0-9975451-0-4
Capolsini P, Andréfouët S, Rion C, Payri C (2003) A comparison of Landsat ETM+, SPOT HRV, Ikonos, ASTER, and airborne MASTER data for coral reef habitat mapping in South Pacific islands. Canadian Journal of Remote Sensing 29:187–200
Chirayath V, Earle SA (2016) Drones that see through waves–preliminary results from airborne fluid lensing for centimeter-scale aquatic conservation. Aquatic Conservation: Marine and Freshwater Ecosystems 26:237–250
Chirayath V, Li AS (2019) Machine learning augmentation and fluid lensing for enhancing coral reef assessment accuracy from remote sensing. IEEE Transactions on Geoscience and Remote Sensing
Collin A, Hench JL (2012) Towards deeper measurements of tropical reefscape structure using the WorldView-2 spaceborne sensor. Remote Sensing 4:1425–1447
Collin A, Archambault P, Planes S (2014) Revealing the regime of shallow coral reefs at patch scale by continuous spatial modeling. Frontiers in Marine Science 1(1):15
Congalton R (1991) A review of assessing the accuracy of classifications of remotely sensed data. Remote Sensing of Environment 37:35–46
Douvere F (2008) The importance of marine spatial planning in advancing ecosystem-based sea use management. Marine Policy 32:762–771
English S, Wilkinson C, Baker V (1997) Survey manual for tropical marine resources. Australian Institute of Marine Science, 390 pp
FGDC (Federal Geodetic Control Subcommittee) (1998) Geospatial positioning accuracy standards part 3: national standard for spatial data accuracy. Report number FGDC-STD-007.2-1998, 25 pp
Callaghan DP, Leon JX, Saunders MI (2015) Wave modelling as a proxy for seagrass ecological modelling: Comparing fetch and process-based predictions for a bay and reef lagoon. Estuarine Coastal and Shelf Science 153:108–120
Gaines SD, Gaylord B, Largier JL (2003) Avoiding current oversights in marine reserve design. Ecological Applications 13:32–46
Ginsburg RP, Alcolado PM, Arias E, Bruckner A, Claro R (2000) Status of Caribbean reefs: initial results from the Atlantic and Gulf reef assessment (AGGRA) program. In: Proceedings of the Ninth International Coral Reef Symposium, Bali, Indonesia, p. 211
Gleason M, McCreary S, Miller-Henson M, Ugoretz J, Fox E, Merrifield M, McClintock W, Serpa P, Hoffman K (2010) Science-based and stakeholder-driven marine protected area network planning: a successful case study from north central California. Ocean and Coastal Management 53:52–68
Glynn PW, Riegl BR, Purkis SJ, Kerr JM, Smith T (2015) Coral reef recovery in the Galápagos Islands: the northern-most islands (Darwin and Wenman). Coral Reefs 34:421–436
Goodman JA, Purkis SJ, Phinn SR (Eds) (2013) Coral Reef Remote Sensing: A Guide for Mapping, Monitoring and Management. Springer, 436 pp, ISBN-10: 9048192919
Graham NA, Jennings S, MacNeil MA, Mouillot D, Wilson SK (2015) Predicting climate-driven regime shifts versus rebound potential in coral reefs. Nature 518:94–97
Graham NA, McClanahan TR, MacNeil MA, Wilson SK, Polunin NV, Jennings S, Chabanet P, Clark S, Spalding MD, Letourneur Y, Bigot L (2008) Climate warming, marine protected areas and the ocean-scale integrity of coral reef ecosystems. PLoS one 3:e3039
Hamylton (2011) A comparison of spatially explicit and classic regression modelling of live coral cover using hyperspectral remote-sensing data in the Al Wajh lagoon, Red Sea. International Journal of Geographical Information Science 26:2161–2175
Hedley JD, Harborne AR, Mumby PJ (2005) Simple and robust removal of sun glint for mapping shallow-water benthos. International Journal of Remote Sensing 26:2107–2112
Hedley JD, Roelfsema CM, Chollett I, Harborne AR, Heron SF, Weeks S, Skirving W, Strong A, Eakin C, Christensen T, Ticzon C (2016) Remote sensing of coral reefs for monitoring and management: a review. Remote Sensing 8:118
Hempson TN, Graham NAJ, MacNeil MA, Hoey AS, Wilson SK (2018) Ecosystem regime shifts disrupt trophic structure. Ecological Applications 28:191–200
Hernández-Cruz LR, Purkis SJ, Riegl BM (2006) Documenting decadal spatial changes in seagrass and Acropora palmata cover by aerial photography analysis in Vieques, Puerto Rico: 1937–2000. Bulletin of Marine Science 79:401–414
Heydari SS, Mountrakis G (2018) Effect of classifier selection, reference sample size, reference class distribution and scene heterogeneity in per-pixel classification accuracy using 26 Landsat sites. Remote Sensing of Environment 204:648–658
Hochberg EJ, Atkinson MJ (2003) Capabilities of remote sensors to classify coral, algae, and sand as pure and mixed spectra. Remote Sensing of Environment 85:174–189
Hughes TP, Barnes ML, Bellwood DR, Cinner JE, Cumming GS, Jackson JB, Kleypas J, Van De Leemput IA, Lough JM, Morrison TH, Palumbi SR (2017) Coral reefs in the Anthropocene. Nature 546:82–90
Jackson JB, Kirby MX, Berger WH, Bjorndal KA, Botsford LW, Bourque BJ, Bradbury RH, Cooke R, Erlandson J, Estes JA, Hughes TP (2001) Historical overfishing and the recent collapse of coastal ecosystems. Science 293:629–637

Jay S, Guillaume M, Minghelli A, Daville Y, Chami M, Lafrance B, Serfaty V (2017) Hyperspectral remote sensing of shallow waters: considering environmental noise and bottom intra-class variability for modeling and inversion of water reflectance. Remote Sensing of Environment 200:352–367

Kerr JM, Purkis SJ (2018) An algorithm for optically-deriving water depth from multispectral imagery in coral reef landscapes in the absence of ground-truth data. Remote Sensing of Environment 210:307–324

Kjerfve B (1986) Comparative oceanography of coastal lagoons. In Wolfe DA. Estuarine Variability, Elsevier, Rockville, Maryland. ISBN 978-0-12-761890-6

Knudby A, Roelfsema C, Lyons M, Phinn S, Jupiter S (2011) Mapping fish community variables by integrating field and satellite data, object-based image analysis and modeling in a traditional Fijian fisheries management area. Remote Sensing 3:460–483

Loubersac L, Burban PY, Lemaire O, Varet H, Chenon F (1991) Integrated study of Aitutaki's lagoon (Cook Islands) using SPOT satellite data and in situ measurements: bathymetric modelling. Geocarto International 6:31–37

Ma Z, Redmond RL (1995) Tau coefficients for accuracy assessment of classification of remote sensing data. Photogrammetric Engineering and Remote Sensing 61:435–439

Mellin C, Andréfouët S, Kulbicki M, Dalleau M, Vigliola L (2009) Remote sensing and fish–habitat relationships in coral reef ecosystems: Review and pathways for multi-scale hierarchical research. Marine Pollution Bulletin 58:11–19

McClenachan L, O'Connor G, Neal BP, Pandolfi JM, Jackson JB (2017) Ghost reefs: Nautical charts document large spatial scale of coral reef loss over 240 years. Science Advances 3:e1603155

Monaco ME, Andersen SM, Battista TA, Kendall MS, Rohmann SO, Wedding LM, Clarke AM (2012) National summary of NOAA's shallow-water benthic habitat mapping of U.S. coral reef ecosystems. NOAA Tech. Memo. NOS NCCOS 122, NCCOS Cent. Coast. Monit. Assess. Biogeogr. Branch, Silver Spring, MD

Mumby PJ, Clark CD, Green EP, Edwards AJ (1998) Benefits of water column correction and contextual editing for mapping coral reefs. International Journal of Remote Sensing 19:203–210

Naseer A, Hatcher BG (2004) Inventory of the Maldives' coral reefs using morphometrics generated from Landsat ETM+ imagery. Coral Reefs 23:161–168

Palumbi SR (2004) Marine reserves and ocean neighborhoods: the spatial scale of marine populations and their management. Annual Review of Environmental Resources 29:31–68

Pandolfi JM, Bradbury RH, Sala E, Hughes TP, Bjorndal KA, Cooke RG, McArdle D, McClenachan L, Newman MJ, Paredes G, Warner RR (2003) Global trajectories of the long-term decline of coral reef ecosystems. Science 301:955–958

Phinn SR, Roelfsema CM, Mumby PJ (2012) Multi-scale, object-based image analysis for mapping geomorphic and ecological zones on coral reefs. International Journal of Remote Sensing 33:3768–3797

Purkis SJ (2005) A "reef-up" approach to classifying coral habitats from IKONOS imagery. IEEE Transactions on Geoscience and Remote Sensing 43:1375–1390

Purkis SJ (2018) Remote sensing tropical coral reefs: The view from above. Annual Review of Marine Science 10:149–168

Purkis SJ, Klemas V (2011) Remote sensing and global environmental change. Wiley-Blackwell, Oxford, UK

Purkis SJ, Myint S, Riegl B (2006) Enhanced detection of the coral Acropora cervicornis from satellite imagery using a textural operator. Remote Sensing of Environment 101:82–94

Purkis SJ, Graham NAJ, Riegl BM (2008) Predictability of reef fish diversity and abundance using remote sensing data in Diego Garcia (Chagos Archipelago). Coral Reefs 27:167–178

Purkis SJ, Harris PM, Ellis J (2012a) Patterns of sedimentation in the contemporary Red Sea as an analog for ancient carbonates in rift settings. Journal of Sedimentary Research 82:859–870

Purkis SJ, Vlaswinkel B, Gracias N (2012b) Vertical-to-lateral transitions among Cretaceous carbonate facies—a means to 3-D framework construction via Markov analysis. Journal of Sedimentary Research 82:232–243

Purkis SJ, Rowlands G, Kerr JM (2015) Unravelling the influence of water depth and wave energy on the facies diversity of shelf carbonates. Sedimentology 62:541–565

Purkis SJ, Kenter JAM, Oikonomou EK, Robinson IS (2002) High-resolution ground verification, cluster analysis and optical model of reef substrate coverage on Landsat TM imagery (Red Sea, Egypt). International Journal of Remote Sensing 23:1677–1698

Purkis SJ, Rowlands GP, Riegl BM, Renaud PG (2010) The paradox of tropical karst morphology in the coral reefs of the arid Middle East. Geology 38:227–230

Purkis, SJ, Dempsey, A, Carlton R, Lubarsky K, Renaud PG (2018) Global Reef Expedition: Cook Islands. Final Report. Khaled Bin Sultan Living Oceans Foundation, Annapolis, MD. Vol. 9: 50p. ISBN: 978-0-9975451-3-5

Purkis, SJ, Dempsey A, Carlton RD, Andréfouët S, Samaniego B, Rauer EM, Renaud PG (2017) Global Reef Expedition: French Polynesia. Final Report. Khaled Bin Sultan Living Oceans Foundation, Annapolis, MD. Vol 5: 80p. ISBN: 978-0-9975451-1-1

Purkis SJ, Kerr J, Dempsey A, Calhoun A, Metsamaa L, Riegl B, Kourafalou V, Bruckner A, Renaud P (2014) Large-scale carbonate platform development of Cay Sal Bank, Bahamas, and implications for associated reef geomorphology. Geomorphology 222:25–38

Riegl BM, Bruckner A, Rowlands G, Purkis SJ, Renaud P (2012) Red Sea coral reef trajectories over 2 decades show increasing community homogenization and decline in coral size. PLoS One 7(5):e38396

Roelfsema CM, Phinn S, Jupiter S, Comley J (2013) Mapping coral reefs at reef to reef-system scales, 10 s–1000 s km2, using object-based image analysis. International Journal of Remote Sensing 18:6367–6388

Roelfsema CM, Lyons M, Kovacs EM, Maxwell P, Saunders MI, Samper-Villarreal J, Phinn SR (2014) Multi-temporal mapping of seagrass cover, species and biomass: a semi-automated object-based image analysis approach. Remote Sens Environ 150:172–187

Roelfsema CM, Kovacs E, Ortiz J, Wolff N, Callaghan DP, Wettle M, Ronan M, Hamylton S, Mumby PJ, Phinn SR (2018) Coral reef habitat mapping: a combination of object-based image analysis and ecological modelling. Remote Sensing of Environment 208:27–41

Rowlands G, Purkis SJ (2015) Geomorphology of shallow water coral reef environments in the Red Sea. Chapter 24 (p. 395–408) In: The Red Sea. The formation, morphology, and environment of a young ocean basin. N. Rasul and I. Stuart (eds.) Springer Publishing, Germany. ISBN 978-3-662-45201-1

Rowlands G, Purkis SJ, Bruckner A (2014) Diversity in the geomorphology of shallow-water carbonate depositional systems in the Saudi Arabian Red Sea. Geomorphology 222:3–13

Rowlands G, Purkis SJ, Bruckner A (2016) Tight coupling between coral reef morphology and mapped resilience in the Red Sea. Marine Pollution Bulletin 105:575–585

Rowlands GP, Purkis SJ, Riegl BM (2008) The 2005 coral-bleaching event Roatan (Honduras): Use of pseudo-invariant features

(PIFs) in satellite assessments. Journal of Spatial Science 53:99–112

Saul S, Purkis SJ (2015) Semi-automated object-based classification of coral reef habitat using discrete choice models. Remote Sensing 7:15894–15916

Sheppard CRC, Ateweberhan M, Bowen BW, Carr P, Chen CA, Clubbe C, Craig MT, Ebinghaus R, Eble J, Fitzsimmons N, Gaither MR (2012) Reefs and islands of the Chagos Archipelago, Indian Ocean: why it is the world's largest marine protected area. Aquatic Conservation: Marine and Freshwater Ecosystems 22:232–261

Spalding MD, Ravilious C, Green EP (2001) World atlas of coral reefs. Univ of California Press

Story M, Congalton R (1986) Accuracy assessment: a user's perspective. Photogrammetric Engineering and Remote Sensing 52:397–399

Stumpf RP, Holderied K, Sinclair M (2003) Determination of water depth with high-resolution satellite imagery over variable bottom types. Limnology and Oceanography 48:547–556

Toonen RJ, Wilhelm TA, Maxwell SM, Wagner D, Bowen BW, Sheppard CRC, Taei SM, Teroroko T, Moffitt R, Gaymer CF, Morgan L (2013) One size does not fit all: the emerging frontier in large-scale marine conservation. Marine Pollution Bulletin 77:7–10

Warren C, DuPont J, Abdel-Moati M, Hobeichi S, Palandro D, Purkis SJ (2016) Remote sensing of Qatar nearshore habitats with perspectives for coastal management. Marine Pollution Bulletin 105:641–653

Wilhelm TA, Sheppard CR, Sheppard AL, Gaymer CF, Parks J, Wagner D, Lewis NA (2014) Large marine protected areas–advantages and challenges of going big. Aquatic Conservation: Marine and Freshwater Ecosystems 24:24–30

Zhang C, Selch D, Xie Z, Roberts C, Cooper H, Chen G (2013) Object-based benthic habitat mapping in the Florida Keys from hyperspectral imagery. Estuarine Coastal and Shelf Science 134:88–97